Schuman, M. D., and D. G. Beshore, *Standardized Distributed Energy Release (SDER) Computer Program*, Final Report, I, AFRPL-TR-78-7, Air Force Rocket Propulsion Laboratory, Edwards AFB, CA (1978).
Smith, I. W., "Kinetics of Combustion of Size-Graded Pulverized Fuels in the Temperature Range 1200-2270°K," *Combustion and Flame*, **17**, 303 (1971).
Smoot, L. D., F. D. Skinner, and R. W. Hanks, "Mixing and Reaction of Pulverized Coal in an Entrained Gasifier," *Amer. Chem. Soc.*, Div. of Fuel Chem. Preprints, **22**, No. 1, 77 (1977).
Stull, D. R., and H. Prophet, *JANAF Thermochemical Tables, 2nd ed.*, National Standard Reference Data System, U.S. Government Printing Office, Washington, DC (1971).
Suuberg, E. M., W. A. Peters, and J. B. Howard, "Product Composition and Kinetics of Lignite Pyrolysis," *Ind. Eng. Chem. Process Des. Dev.*, **17**, 37 (1978).
Svehla, R. A., *Estimated Viscosities and Thermal Conductivities of Gases at High Temperatures*, NASA TR R-132, Nat. Aeronautics and Space Adm., Washington, DC (1962).
Ubhayakar, S. K., D. B. Stickler, and R. E. Gannon, "Modelling of Entrained-Bed Pulverized Coal Gasifiers," *Fuel*, **56**, 281 (1977).
Wen, C. Y., and T. Z. Chaung, "Entrainment Coal Gasification Modeling," *Ind. Eng. Chem. Process Des. Dev.*, **18**, 684 (1979).
Wender, I., "Catalytic Synthesis of Chemicals From Coal," *Amer. Chem. Soc.*, Div. of Fuel Chem. Preprints, **20**, No. 4, 16 (1975).
Williams, F. A., *Combustion Theory*, Addison-Wesley, Reading, MA (1965).

Manuscript received November 20, 1979; revision received April 21, and accepted May 7, 1980.

Studies in the Synthesis of Control Structures for Chemical Processes:

Part IV. Design of Steady-State Optimizing Control Structures for Chemical Process Units

YAMAN ARKUN
and
GEORGE STEPHANOPOULOS
Dept. of Chemical Engineering and Materials Science
University of Minnesota
Minneapolis, MN 55455

The design of the steady-state optimizing control for a single unit is formulated within the framework of the nonlinear mathematical programming theory. Alternative implementational strategies are developed and a multilevel screening procedure is proposed to arrive at the best optimizing control configuration. Numerical examples on a fluid catalytic cracking unit and a distillation column demonstrate the systematic design and the synthesis of the most promising optimizing control structures for these systems.

SCOPE

One of the most challenging tasks for a chemical engineer is to design a chemical process that would operate safely in the most profitable fashion to achieve certain design objectives. Subject to varying market conditions, changing raw materials, different product specifications, and other external disturbances, the chemical plant should operate smoothly over a broad range of operating regimes to stay feasible and profitable. The existence of such a dynamic environment around an operating chemical plant necessitates the existence of well designed control structures to maintain or improve the plant operation on-line, in terms of economics, regulation, reliability, and safety aspects.

Control objectives for a chemical process originate from certain regulation tasks (i.e., product quality control, material balance control, safety, environmental regulations, etc.) and economic objectives (i.e., optimizing the economic performance). Such a classification of control objectives automatically formulates the different design activities for the regulatory and optimizing control structures. Whereas regulatory objectives require certain variables to be kept at specified set-points or within permissible bounds, economic objectives will call for optimizing control actions. In the presence of different types of disturbances, optimal set-point values for the controllers have to be determined, and the necessary set-point changes have to be implemented on-line.

In the previous process control structure synthesis methods (Buckley, 1964; Govind and Powers, 1976; Douglas, 1977; Umeda et al. 1978), the distinction between the different classes of control objectives and its impact on the design of the plant control structure have not been addressed. Articles representing the industrial views have recently indicated that, the steady-state optimizing control constitutes the most fruitful

Y. Arkun is presently with the Dept. of Chemical and Environmental Engineering, Rensselaer Polytechnic Institute, Troy, N.Y., 12181.

0001-1541-80-4211-0975-$01.65.

control practice in the chemical process industry (Latour, 1976; Ellingsen, 1976; Barkelew, 1976; Lee and Weekman, 1976), whereas regulation of the chemical process units is accomplished by the practicing engineers with satisfactory degree of acceptance. Especially in chemical units processing large throughputs such as those found in the petrochemical industry, the economic incentive for steady-state optimization is strongly felt (Kaiser, et al. 1966; Lee and Weekman, 1976).

Nevertheless, there has been no systematic approach towards the design and implementation of optimizing control structures. In the absence of any theoretical foundations and practical ramifications, the designer relies on his operating experience and intuition to select an optimizing control policy without exploring all the viable alternatives. This paper will lay down the theoretical foundations for the synthesis and design of steady-state optimizing control structures for chemical processes. The implementational problems will be also addressed to develop practical control strategies for the on-line application of the optimizing controllers.

Optimum design of chemical processes dictates that the optimal operating point of a well-designed plant lies at the intersection of operating constraints (Lee and Weekman, 1976; Rijnsdorp, 1967; Maarleveld and Rijnsdorp, 1970; Baxley 1969; Kaiser et al. 1966; Kuehn and Davidson, 1961; Shah, 1970; Ishida, 1975). Furthermore, current industrial practice indicates that the optimal operating point switches from the intersection of one set of active constraints to another as process disturbances change with time (Lee and Weekman, 1976; Davis et al. 1974; Maarleveld and Rijnsdorp, 1970; Duyfjes et al. 1973; Ishida 1975, Webb et al. 1977). Such a dynamic evolution of the process operation constitutes the major thrust for the successful implementation of an optimizing control strategy.

CONCLUSIONS AND SIGNIFICANCE

The problem of designing the most appropriate optimizing control configuration for a given processing unit has been formulated within the Kuhn-Tucker theory of mathematical programming. Such formulation allows the designer: (1) to follow the move of the design operational constraints when the values of the external disturbances change, and to identify the set of active constraints which determine the new optimum; (2) to identify the alternative initial control strategies to guarantee operational feasibility; (3) to develop the alternative optimizing control routes that will lead the plant to the new optimum operation; and (4) to screen these routes and select the most appropriate for the particular process.

The screening of the alternative optimizing control strategies is implemented within an imbedded branch and bound policy which is used at various levels of sophistication. Starting with simple engineering considerations like safety and bottlenecking, several alternatives are rejected. On the second level, static considerations like steady-state gains and static interaction among the loops are included. In the final level, the time delays, time constants, and dynamic interactions among the loops are considered.

The overall approach lends itself rather easily to a systematic synthesis of the best optimizing control configuration and a rigorous design of the resulting operation. Unlike the previous attempts the present work is general and can be applied to any unit of arbitrary complexity.

The numerical examples on two processing units, i.e., a fluid catalytic cracker and a distillation column, demonstrate the value of the proposed approach in designing an optimizing control policy for a variety of external disturbances. They also reveal the problems of feasibility and optimality connected to the operation of these two systems and how to approach them in a rigorous and systematic manner.

PROBLEMS OF OPTIMIZING CONTROL

Consider a continuous stirred tank reactor with a first-order, endothermic reaction $A \rightarrow B$ (Arkun, 1979). During normal operation, the reactor holdup V, temperature T, and the exit concentration of the reactant, C_A, are constrained by specified design limits V_m, T_m, and C_{Am} respectively. Figure 1 shows the feasible operating regions and the location of the optimum steady-state operations for different values of the feed temperature. As feed disturbances such as flowrate, concentration, temperature, or economic disturbances like the specific heating cost and product value vary, different sets of active constraints will determine the location of the optimum operating point. Consequently, any optimizing control should: (1) identify and monitor the set of active constraints which uniquely determine the optimum, and (2) try to move the process to this optimum by making the necessary set-point adjustments.

A similar situation has been presented by Maarleveld and Rijnsdorp (1970) for the optimizing control of distillation columns. The operating constraints for a deisopentanizer are illustrated in Figure 2. As the column throughput increases, the feasible area changes due to the motion of the constraints, and the optimum is defined by the intersection of different constraints. Originally the optimum is at the intersection of the condenser and the feed preheater constraints, Figure 2(a). As the feed flowrate increases, the optimum operation eventually switches to the intersection of the two flooding constraints, Figure 2(c). The original optimum operating point becomes not only suboptimal, but more importantly, it dictates an infeasible operational policy (i.e., the trays become overloaded). Hence, the desired optimizing control structure for this column must retain and achieve feasible optimum operation.

The above two qualitative examples define a set of problems which should be resolved by any well-organized optimizing control structure. These problems will be described qualitatively in this section and will be formulated rigorously in the next.

1. Optimizing control structures will be needed as long as there exists a spectrum of disturbances entering the process. Classification of the disturbances in terms of their frequency and economic impact is essential to decide when to reoptimize the process operation. First of all, reoptimization will be considered only in the presence of persistent "slow" disturbances acting on a process with relatively faster dynamics. Only under such conditions, the process can be considered at steady or pseudo-steady state so that steady-state optimization becomes valid and meaningful. The final decision for reoptimization will be based on economic considerations which are guided by the classification of the persistent "slow" disturbances according to their economic impact. Since new set-point changes towards the optimum will introduce upsets in normal operation, the economic incentive will be of paramount importance.

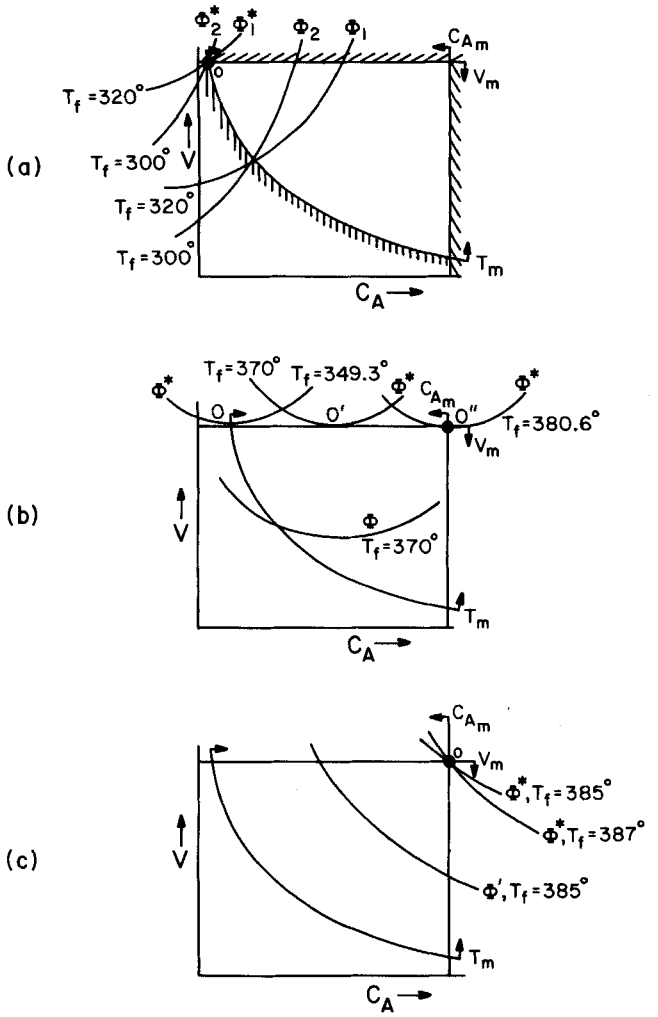

Figure 1. Effect of feed disturbances on optimal operation of a CSTR.

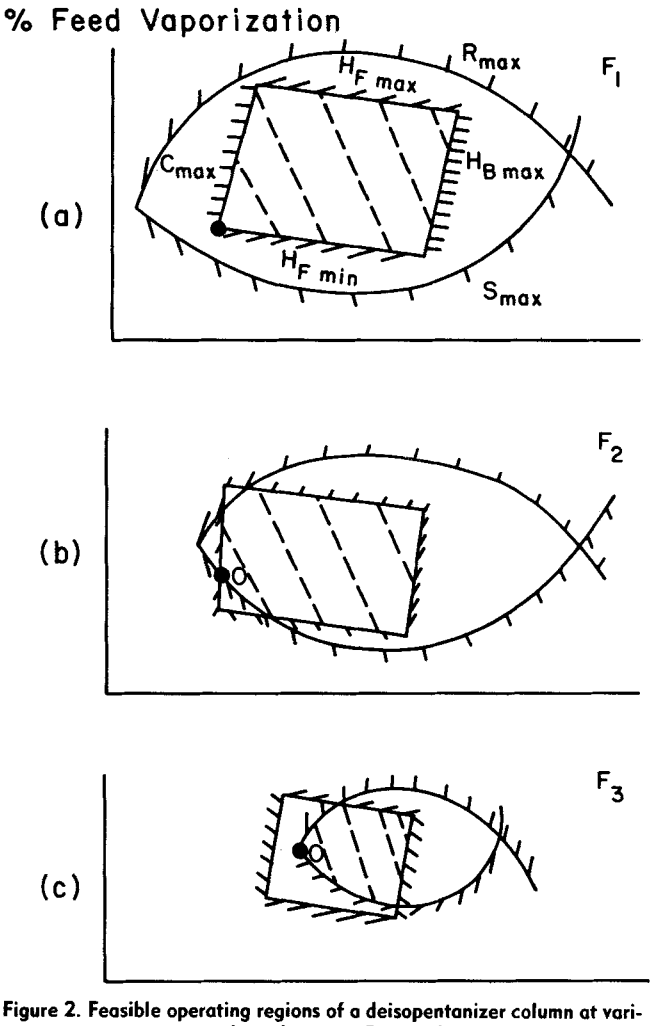

Figure 2. Feasible operating regions of a deisopentanizer column at various throughputs, F. $F_3 > F_2 > F_1$.

2. In the past and present industrial practice, most of the attention has been focused on determining the optimal operating point within the general discipline of planning. Little attention has been paid to the process operation itself such as how to accomplish the reoptimization through the existing control loops. It is clear from the reactor example that the optimum switches to the intersection of different set of constraints; but the question of how to move the operation to the new optimum by the controllers still has to be systematically answered.

Any reoptimization manifests itself through a sequence of set-point changes of controllers and how to select the best sequence remains the important question to be tackled in this paper.

3. The operational process constraints constitute a very central and basic element of an optimizing control strategy for the following reasons. (a) The optimum operation of a well-designed plant is usually found at the intersection of operational constraints. (b) These constraints move as the disturbances change value. (c) The constraints which define the optimum operation change as the disturbances change, thus resulting in different regulatory controllers. A well-conceived optimizing control structure should account for the above characteristics.

4. Any model-based optimizing control should address directly the problem of the inaccuracies in the model and its parameters. The design strategy to be developed in the subsequent sections is to a large extent model independent and uses only process measurements.

In the following sections we will tackle all the above problems in an attempt to develop the theoretical foundations and the implementational strategies for the synthesis and design of optimizing control structures for chemical processes.

ANALYSIS OF THE PROBLEM'S CHARACTERISTICS

We will consider a given process unit as a self-standing plant with a well-defined economic objective. (Problems concerning the optimizing control of a large-scale system of interacting units will be treated in a forthcoming publication.) The optimization problem for the single unit is to determine the optimal operating point when the values of a set of external disturbances change.

Steady-State Optimization Problem

For a set of slowly varying external disturbances, we assume that the process is at pseudosteady state. Then, the following static optimization problem can be formulated.

$\min_m \Phi(x, m, d)$	Objective Function
(P_1) subject to:	
$g'(x, m, d) = o$	System's State Equations
$g''(x, m, d) \leq b$	Process Design Constraints
$r(x, m, d) = r_d$	Regulatory Control Tasks
$-d + d^* = o$	Disturbance Specifications

where x is the vector of states; m is the vector of manipulated variables; and d is the vector of nonstationary, "slow" disturbances with major economic impact on the optimal process operation. For the classification of disturbances and the identification of the corresponding regulatory and optimizing control tasks, the reader should refer to Morari, et al. (1978). The inequality design constraints represent limits on process variables such as those resulting from operational requirements, safety considerations, product purity limits, etc. Active con-

straints $r(x, m, d) = r_d$ are imposed by the regulatory objectives which have to be always satisfied (i.e., fixed production rate, product quality specifications, etc.).

Classification of Constraints at Design Optimum

At the calculated optimum $X^* = (x^*, m^*, d^*)$ of the above problem (P_1), some of the inequality constraints will be active. Consequently, the following set of equations will hold at the optimum steady state;

$$(L_{P_1}) \quad \begin{aligned} & g'(x, m, d) = 0 \\ & r(x, m, d) = r_d \\ & g_A(x, m, d) = b_A \\ & g_{IA}(x, m, d) < b_{IA} \\ & -d + d^* = 0 \end{aligned}$$

where

$$g'' = \begin{bmatrix} g_A\text{: Set of Active Design Constraints} \\ g_{IA}\text{: Set of Inactive Design Constraints} \end{bmatrix}$$

Classification of the constraints as active and inactive at the current optimum will now guide us in the synthesis of optimizing control structures as we proceed with the selection of controlled variables.

Selection of Process Controlled Variables

The regulatory control objectives and the active design constraints at the current optimum will constitute the class of primary controlled variables denoted by c^P as:

$$[c^P(x, m, d)] = \begin{bmatrix} r(x, m, d) \\ g_A(x, m, d) \end{bmatrix} = \begin{bmatrix} c^P_{\text{reg}} \\ c^P_{\text{opt}} \end{bmatrix}$$

The primary controlled variables c^P are to be regulated at their current optimum set points in the presence of fast changing disturbances through the development of appropriate control loops. This approach will be called the "active constraints control."

Instead of controlling the active constraints at the optimum, we could have chosen to regulate some other process variables at their optimum values as determined by the set of constraints (L_{P_1}).

To illustrate the difference between the above two approaches, let us consider the two-dimensional problem in Figure 3. There are four constraints that should be satisfied: c_1, c_2, c_3, and c_4. Let the steady-state optimum for a given value of the disturbances be at the point B. Following the active constraints control approach, we could regulate point B by controlling the active constraints c_3 and c_4 (whose intersection determines point B). Instead, we could maintain operation at the point B by controlling the two inactive constraints c_1 and c_2 at their corresponding set-points, $\bar{c}_1$ and $\bar{c}_2$.

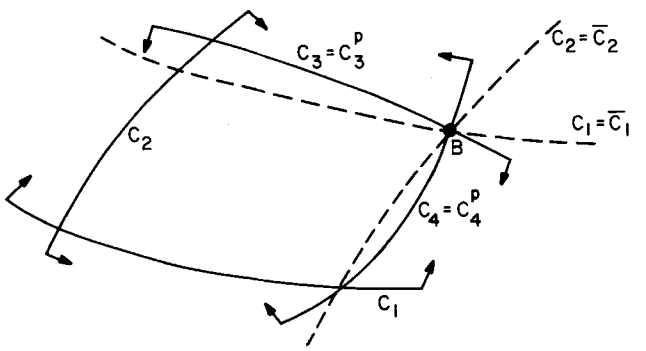

Figure 3. Alternative controlled variables at steady-state optimum B.

The active constraints control approach will be preferred for the following reasons.

1. If the active constraints are controlled, we have a direct hold on the operational variables of immediate interest (avoid violation of constraints).
2. If the active constraints are regulated, on-line optimization may be eliminated for a certain set of disturbances. This will be true if the same set of constraints determines the optimum for some range of the disturbances' values, i.e., when $d \in D_i$. This feature has also been called the "Invariability Condition" by Findeisen (1976). In this case, a simple feedback control structure regulating the same set of active constraints at given set-points will guarantee optimality.
3. By a first-order perturbation analysis, it can be shown (Arkun, 1979) that the constraints will move in response to a change in the value of the disturbances. This movement generates the possibility of infeasible operation. By regulating the active control constraints, we can avoid infeasibilities. This is not very easy, if the control is based on the regulation of the inactive constraints.
4. Returning to the example of Figure 3, we notice that the successful regulation of the inactive constraints c_1 and c_2 at their values $\bar{c}_1$ and $\bar{c}_2$ depends on the goodness of the mathematical models describing c_1 and c_2. On the other hand, the control of the active constraints c_3 and c_4 can be accomplished successfully using direct process measurements independent of any model.

Selection of Manipulated Variables

We will choose the primary controlled variables c^P as the measurements of the control loops. If any of the elements of c^P are unmeasured, we will replace them with "secondary" measurements. For the selection of the appropriate secondary measurements to estimate the unmeasured primary variables, the reader is referred to the work of Weber and Brosilow (1972), Morari (1977), and Joseph and Brosilow (1978).

After the measurements have been identified, the manipulated variables have to be selected to compose the regulatory control structure. The algorithm by Morari (1977), which uses the extended structural controllability and observability concepts, is employed to generate alternative feasible regulatory control structures. As a result, a proper subset of manipulated variables m_D is selected to control c^P.

Partition the vector of the selected manipulated variables as,

$$m^T = [m_D^T \tilde{m}^T] \text{ with } \dim(m_D) = \dim c^P$$

The available extra degrees of freedom at the optimum for $d = d^*$ are:

$$\dim(\tilde{m}) = \dim(m) - \dim(c^P)$$

Effect of Disturbances on Optimal Operation

Most of the time, the process units will be subject to persistent disturbances with economic impacts such as feedstock changes. These disturbances would move the current optimum to a different point where different sets of constraints will be active.

Consider the set of constraints (L_{P_1}) at the current optimum X^* as:

$$(L^*_{P_1}) \quad \begin{aligned} & g'(x^*, m^*_D, \tilde{m}^*, d^*) = 0 \\ & c^P(x^*, m^*_D, \tilde{m}^*, d^*) - c^P_d = 0 \\ & -d + d^* = 0 \\ & g_{IA}(x^*, m^*_D, \tilde{m}^*, d^*) - b_{IA} < 0 \end{aligned}$$

Let us consider that disturbances deviate significantly from their design values d^* to affect the optimal operating point. The following options would be considered as alternative optimizing control strategies.

i) Together with m_D, use $\tilde{m}$ for feedback optimizing control

selecting some additional secondary controlled variables c^s to use up the available degrees of freedom. Selection of c^s can be done according to the criteria given by Morari et al. (1978).

ii) Use $\tilde{m}$ in feed forward optimization.

iii) Use all degrees of freedom available to move towards the new optimum. In other words, change set-points c_d^P and $\tilde{m}$.

The first and second optimizing control strategies will exist, only if there exists free $\tilde{m}$. Otherwise, the tight constraints c^P will form the feedback optimizing control structure together with its manipulated variables m_D. Quite often the optimum will lie at the intersection of as many constraints as there are degrees of freedom leaving no $\tilde{m}$ available for implementing strategies (i) and (ii) above (Maarleveld and Rijnsdorp, 1970; Westerberg, 1973b).

When the optimum moves considerably with disturbances, feedback optimizing control will either lead to infeasible operation or cause large deterioration in the economic objective as compared to the third option. The displacement of the optimum from one set of constraints to another, due to the change in the values of economic disturbances, necessitates the design of an optimizing control structure that will change the operating point rather than merely keeping it at the initial design optimum. In the following sections, we will develop the theoretical foundations towards the construction of such optimizing control structures.

CONTROL OF CONSTRAINTS: THEORETICAL DEVELOPMENTS

This section deals with the application of the Kuhn Tucker theory of nonlinear mathematical programming in the synthesis of the optimizing control structures for a processing unit. The extension of this development to large-scale integrated systems can be found in Arkun (1979) and will be presented in a forthcoming publication.

For the set of constraints (L_{P_1}) at the design optimum, let us define.

$$\bar{x} = \begin{bmatrix} x \\ d \\ m_D \end{bmatrix} \text{ and } f = \begin{bmatrix} g'(\bar{x}, \tilde{m}) \\ c^P(\bar{x}, \tilde{m}) - c_d^P \\ -d + d^* \end{bmatrix}$$

(Lumped active constraints)

where

$$c^P \equiv \begin{bmatrix} c^P_{\text{reg}} \\ c^P_{\text{opt}} \end{bmatrix} = \begin{bmatrix} r(\bar{x}, \tilde{m}) \\ g_A(\bar{x}, \tilde{m}) \end{bmatrix}$$

Lagrangian Formulation and Kuhn-Tucker Conditions

Formulate the Lagrangian function for the problem (P_1):

$$L(x, m, \lambda) = \Phi(\bar{x}, \tilde{m}) - \lambda^T f(\bar{x}, \tilde{m}) - \lambda_{IA}^T g_{IA}(\bar{x}, \tilde{m})$$

where λ is the vector of Lagrange multipliers for the equality constraints $f(\bar{x}, \tilde{m}) = 0$; and λ_{IA} is the vector of Kuhn-Tucker multipliers for the inactive design constraints $g_{IA}(\bar{x}, \tilde{m}) < 0$.

The Kuhn-Tucker conditions for the minimum are,

$$\nabla_{\bar{x}} L = \frac{\partial \Phi}{\partial \bar{x}} - \frac{\partial f^T}{\partial \bar{x}} \lambda - \frac{\partial g_{IA}^T}{\partial \bar{x}} \lambda_{IA} = 0 \quad (1)$$

$$\nabla_{\tilde{m}} L = \frac{\partial \Phi}{\partial \tilde{m}} - \frac{\partial f^T}{\partial \tilde{m}} \lambda - \frac{\partial g_{IA}^T}{\partial \tilde{m}} \lambda_{IA} = 0 \quad (2)$$

and

$$\lambda_A^T (g_A - b_A) = 0$$

$$\lambda_{IA}^T (g_{IA} - b_{IA}) = 0$$

$$\begin{bmatrix} \lambda_A \\ \lambda_{IA} \end{bmatrix} \leq 0$$

$$g''(\bar{x}, \tilde{m}) \leq b$$

$$r(\bar{x}, \tilde{m}) - r_d = 0$$

$$-d + d^* = 0$$

$$g'(\bar{x}, \tilde{m}) = 0$$

Hence, at the optimum X^*:

$$g_A = b_A, \; g_{IA} < b_{IA}$$

Furthermore,

$$\lambda_{IA} = 0 \quad (3)$$

That is, the vector of Kuhn-Tucker multipliers for the inactive inequality constraints is zero. Also,

$$\lambda_A < 0 \quad (4)$$

That is, Kuhn-Tucker multipliers for the active design constraints are negative.

Eq. 1 gives the lagrange multipliers

$$\lambda^T = \frac{\partial \Phi}{\partial \bar{x}^T} \left[\frac{\partial f}{\partial \bar{x}^T} \right]^{-1} \equiv \frac{\partial \Phi}{\partial \bar{x}^T} J^{-1} \quad (5)$$

Substituting λ into Eq. 2, one obtains the constrained derivatives:

$$\left(\frac{\partial \Phi}{\partial \tilde{m}^T} - \frac{\partial \Phi}{\partial \bar{x}^T} J^{-1} \frac{\partial f}{\partial \tilde{m}^T} \right) \equiv \left(\frac{\partial \Phi}{\partial \tilde{m}^T} - \frac{\partial \Phi}{\alpha \bar{x}^T} J^{-1} C \right) = 0 \quad (6)$$

A physical interpretation for any Kuhn-Tucker multiplier $\lambda_{A,i}$ is given by Westerberg and DeBrosse (1973b). Kuhn-Tucker multiplier $\lambda_{A,i}$ is the ratio of the change in the objective function Φ to an infinitesimal change in the value of the constraint $g_{A,i}$, holding all the other constraints and decision variables unchanged. Hence, the sign of the Kuhn-Tucker multipliers shows us how Φ will change with a movement to the interior of the feasible region of an active constraint. For example, $\lambda_{A,i} < 0$ denotes that an infinitesimal move to the interior of $g_{A,i}$, holding other constraints tight, will increase Φ.

Development of Initial Search Direction (ISD)

Consider that while the process is operating at the optimum point X^*, the disturbances change and the corresponding optimal operating point lies at the intersection of a different set of process constraints.

The current optimum X^* will now constitute a starting point to develop the search direction and with that the control policy to initiate the search towards the new optimum. Since it is no longer profitable to hold all the active constraints c^P tight at their set-points c_d^P, we will release a proper subset of these constraints to use as our search coordinates.

To identify the new search direction one should evaluate the Kuhn-Tucker multipliers at a feasible point, after the disturbances change to their new values. As the first step to construct the initial search direction, we look at the problem of finding a feasible point corresponding to the new disturbance values.

Finding a Feasible Operating Point, X°

Consider that $d = d' = d^* + \delta d$; i.e., slow disturbances with economic impacts deviate from their design values. We need to find a feasible operating point for the following set of equations.

$$(L') \quad \begin{array}{l} g'(x, m_D, \tilde{m}, d') = 0 \\ \text{System Equations} \\ c^p_{\text{reg}}(x, m_D, \tilde{m}, d') - c^p_{d,\text{reg}} = 0 \\ \text{Regulatory Control Constraints} \\ c^p_{\text{opt}}(x, m_D, \tilde{m}, d') - c^p_{d,\text{opt}} \leq 0 \\ \text{Currently Controlled Active Constraints} \\ g_{IA}(x, m_D, \tilde{m}, d') \leq b_{IA} \\ \text{Inactive Inequality Constraints at Current Optimum} \end{array}$$

Modification of Constraint Sets at X°

At the calculated feasible point:

$$X^\circ = \begin{bmatrix} x^\circ \\ d' \\ m_D^\circ \end{bmatrix}$$

that satisfies the above set of constraints (L'), some of the inactive constraints g_{IA} will become active as:

$$g_{IA} = \begin{bmatrix} g'_{IA} - b'_{IA} = 0 \\ \tilde{g}_{IA} - \tilde{b}_{IA} < 0 \end{bmatrix}$$

Since new active constraints g'_{IA} are introduced, some of the previously active constraints c^p_{opt} will become inactive to preserve the determinacy features of the system as:

$$c^p_{\text{opt}} = \begin{bmatrix} c'^p_{\text{opt}} - c'^p_{d,\text{opt}} = 0 \\ \tilde{c}^p_{\text{opt}} - \tilde{c}^p_{d,\text{opt}} < 0 \end{bmatrix}$$

Starting at the current optimum X^* *where* c^p_{opt} is the set of active inequality constraints:

i) Release $\tilde{c}^p_{\text{opt}} \in c^p_{\text{opt}}$

where $\tilde{c}^p_{\text{opt}}$: constraints that will not become active at the feasible point X°.

ii) Keep $c'^p_{\text{opt}} \in c^p_{\text{opt}}$ tight

where c'^p_{opt}: constraints that remain active at X° after d changes.

Partitioning of Initial Constraint Control Loops

1) The controlled variables $\tilde{c}^p_{\text{opt}}$ that are *released* will identify the initial *servo loops* for which the set-points $\tilde{c}^p_{d,\text{opt}}$ will be changed by moving into their feasible regions.

2) The controlled variables c'^p_{opt} that are kept *tight* on their bounds will define the *regulatory* loops as:

$$c^p_{\text{opt}} \begin{cases} \nearrow \tilde{c}^p_{\text{opt}} \rightarrow \text{Servo Loops} \\ \searrow c'^p_{\text{opt}} \rightarrow \text{Regulatory Loops} \end{cases}$$

The feasible point will be attained by changing set-points $\tilde{c}^p_{d,\text{opt}}$ of the servo loops, while keeping c'^p_{opt} and c^p_{reg} tight by the regulatory loops.

Control Structure Modification at X°

At the feasible point X°, new constraints g'_{IA} will become active. These active constraints will constitute the new control objectives and together with the tight constraints c'^p_{opt}, c^p_{reg} make up the new set of controlled variables, c^p. Redefining the set of active constraints at X° we have,

$$c^p = \begin{bmatrix} c^p_{\text{reg}}(x, m_D, \tilde{m}, d) \\ c'^p_{\text{opt}}(x, m_D, \tilde{m}, d) \\ g'_{IA}(x, m_D, \tilde{m}, d) \end{bmatrix}$$

and thus we determine the new primary controlled variables composed of regulatory objectives and the new active inequality constraints at X°.

We are no longer interested in controlling $\tilde{c}^p_{\text{opt}}$ which have moved into their feasible region at X°. Instead, the new active constraints become our critical variables to be controlled on their bounds. The manipulated variables which have been used to control $\tilde{c}^p_{\text{opt}}$ will now be candidates to control g'_{IA}.

Restructuring the controlled variables c^p, alternative feasible control structures can be generated at X° through the algorithm given by Morari (1977), as it was done at the design optimum X^*.

Selection of New Search Directions (NSD) at X°

While feasible operation is attained through the initial search direction after disturbances change, the second phase of the optimizing control actions is to find new search directions towards the new optimum.

Redefining the new set of lumped active constraints f at X°,

$$f = \begin{bmatrix} g'(x, m_D, \tilde{m}, d') \\ c^p(x, m_D, \tilde{m}, d') - c^p_a \end{bmatrix}$$

the variations around X° yield:

$$\delta f = \frac{\partial f}{\partial \tilde{x}^T}\delta\tilde{x} + \frac{\partial f}{\partial \tilde{m}^T}\delta\tilde{m} = \tilde{J}\delta\tilde{x} + C\delta\tilde{m} \tag{7}$$

$$\delta\Phi = \frac{\partial\Phi}{\partial \tilde{x}^T}\tilde{J}^{-1}\delta f + \left(\frac{\partial\Phi}{\partial \tilde{m}^T} - \frac{\partial\Phi}{\partial \tilde{x}^T}\tilde{J}^{-1}C\right)\delta\tilde{m} \tag{8}$$

where $\tilde{x}^T = [x^T m_D^T]$.

Substituting

$$\delta f = \begin{bmatrix} 0 \\ \delta c^p_{\text{opt},d} \end{bmatrix}$$

into Eq. 8 we take,

$$\delta\Phi = \lambda_A^T\delta c^p_{\text{opt},d} + \left(\frac{\partial\Phi}{\partial \tilde{m}^T} - \frac{\partial\Phi}{\partial \tilde{x}^T}J^{-1}C\right)\delta\tilde{m}$$

$$= \lambda_A^T\delta c^p_{\text{opt},d} + \beta^T\delta\tilde{m} \tag{9}$$

where, λ_A is the vector of Kuhn-Tucker multipliers for the new set of active constraints at X° and β denotes the constrained sensitivity of Φ with respect to $\tilde{m}$ at X°.

Criterion to Select NSD

Evaluate $\lambda_{A,i}$ "Kuhn-Tucker Multipliers"

$$\lambda_{A,i} = \frac{\delta\Phi}{\delta c^p_{i,\text{opt},d}}\, i = 1, \ldots \dim c^p_{\text{opt}}$$

1) If $\lambda_{A,i} < 0$, keep $c^p_{i,\text{opt}}$ tight; and 2) If $\lambda_{A,i} > 0$, release $c^p_{i,\text{opt}}$.

Selection of new search direction will lead to the modification of control loops as follows.

Repartitioning of Control Loops

$c^p_{\text{opt}} = [c^p_T \,\vdots\, c^p_R]$

c^p_T: Tight constraints which will identify new regulatory loops.

c^p_R: Released constraints which will identify the new servo loops.

Search Procedure towards New Optimum

After the new search directions are found, the initial optimization problem (P_1) for the new values of the disturbance (i.e., $d \neq d^*$) can now be casted into:

$$(P_2)\quad \begin{aligned} &\text{Min } \Phi(c^p_{R,d}, c^p_{T,d}, c^p_{\text{reg},d}, \tilde{m}) \\ &s.t \\ &\quad g_{IA}(c^p_{R,d}, c^p_{T,d}, c^p_{\text{reg},d}, \tilde{m}) - b_{IA} \leq 0 \end{aligned}$$

The set-points of the released constraints $c^p_{R,d}$ and $\tilde{m}$ (if available) are the only free variables to adjust at each optimization step. Equality constraints f will be satisfied at each optimization step determining the values of the dependent variables x, m_D together with g_{IA} and Φ. Hence, the search algorithm assumes the existence of a method of solving a set of design equations such as considered by Westerberg and DeBrosse (1973a, 1973b).

Interruption of Search

As the set-points $c^p_{R,d}$ and $\tilde{m}$ are changed, some of the inactive constraints g_{IA} will become active (i.e., $\tilde{g}_{IA} = \tilde{b}_{IA}$). This will interrupt the search, since any further set-point change in $c^p_{R,d}$ will violate the constraints $\tilde{g}_{IA}$. The following changes in the

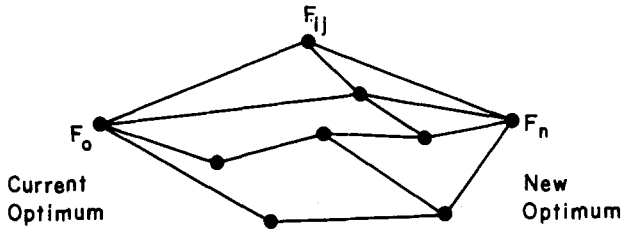

Figure 4. Optimizing control sequencing paths.

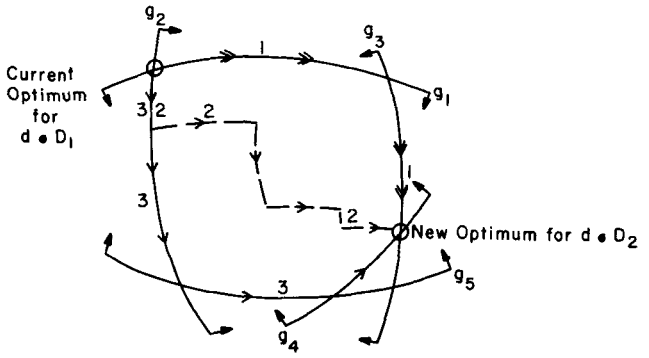

Figure 5. Example demonstrating alternative operational routes.

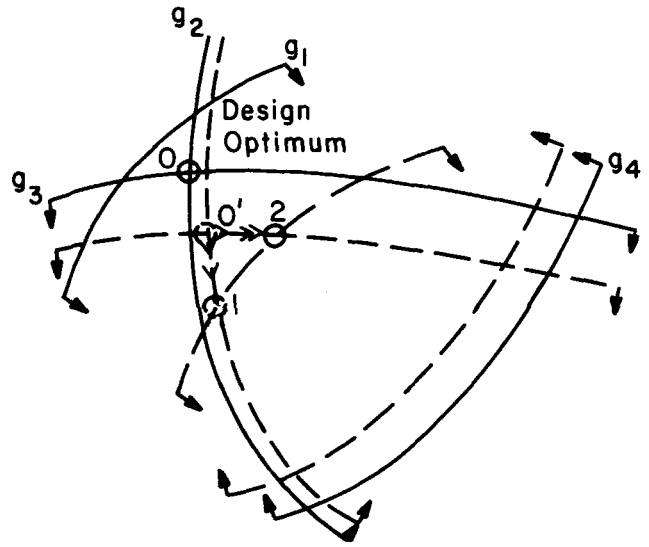

Figure 6. Alternative feasible points and ISD's after a disturbance entered a unit.

current control structure will have to be made to accommodate the new control objectives, $\bar{g}_{IA}$.

Control Structure Modification (Arkun, 1979)

i) Transform $\bar{g}_{IA}$ into the set of tight constraints and control it at set-points $\bar{b}_{IA}$.

ii) Exclude $\dim(\bar{g}_{IA})$ controlled variables $\tilde{c}_R^p$ from the set of released constraints c_R^p:

Partition

$$c_R^p = [\bar{c}_R^p \vdots \tilde{c}_R^p] \ .$$

$\tilde{c}_R^p$ will now become dependent variables assuming values inside their feasible region and they cannot be adjusted freely any more as search coordinates. The manipulated variables which used to control $\tilde{c}_R^p$ are now free and can be utilized to control the new controlled variables $\bar{g}_{IA}$.

iii) Redefine the tight, released and inactive constraints as:

$$\hat{c}_T^p = [c_T^p, \tilde{g}_{IA}] \Rightarrow \text{New Regulatory Loops}$$

$$c_R^p = \bar{c}_R^p \qquad \Rightarrow \text{New Servo Loops}$$
$$g_{IA} = [\bar{c}_R^p, \tilde{g}_{IA}] \ .$$

The search is continued by the reduced set of search directions c_R^p. Whenever new constraints become active at a search step of the optimization problem (P_2), constraint sets are modified accordingly to define the regulatory and the servo loops. If there remains no search direction at a search point due to encountering new constraints, Kuhn-Tucker multipliers are re-evaluated at that point. If they are all negative, an apparent minimum is found and the search is terminated; otherwise, it is continued with the new search direction selected.

IMPLEMENTATIONAL STRATEGIES

In the previous section, a constrained steady-state optimization problem was solved, using the Kuhn-Tucker theory of nonlinear programming. The solution algorithm points to the development of alternative practical control strategies for the on-line implementation of the optimizing controllers. Implementational problems will have to be addressed explicitly to design optimizing control structures satisfying the practical needs of any existing process. The following sections outline what these needs are and how acceptable optimizing control strategies can be generated within the context of the mathematical theory we have already developed.

Sequencing Problem

Given the current operating point and the new optimum, the goal of any optimizing control policy is to bridge the gap between these two points. Such an overall plant goal has to be translated to the operational objectives of the control loops, in order to be meaningful and feasible. Any reoptimization will have to be accomplished through a *sequence* of set-point changes of the control loops. The optimizing control theory and the search procedure as developed earlier have delineated the sequencing strategies to be followed. After we develop the search coordinates as defined by the released and tight constraints, we can directly identify an operational route between two operating points.

Consequently, a sequencing tree composed of alternative routes to the new optimum can be constructed as shown in Figure 4. Each node F_{ij} represents an intermediate operating point (i.e., a search point in the optimization procedure) with a set of constraints to be controlled by the manipulated variables. Moreover, each branch between two nodes uniquely describes the control action (i.e., regulatory and optimizing) taken by the current control structure. As a result, each path between the initial and the final node will represent a different sequence of control actions (i.e., regulatory feedback structures and set-point changes). Alternative routes will exist because movement along alternative sets of constraints can lead to the optimum (Figure 5).

For this example, the Kuhn-Tucker multipliers for the currently active constraints g_1 and g_2 would dictate that they should both be released to improve the objective. However, the sequence of set-point changes will be an implementational decision variable that leads to the generation of alternative operational routes. The objective for the generation of alternative sequences will be, like any other synthesis problem (i.e., synthesis of control structures, heat exchanger networks, and separation sequences) not to exclude any attractive structures. We will now give special emphasis to the generation of initial branches, since they pose some important feasibility problems.

Generation of Initial Branches

The search procedure exercised by the optimizing controllers has two distinct phases. The first phase consists of finding a feasible point and making the necessary set-point changes to reach it through the initial search directions (ISD). The second

phase is concerned with the optimality besides the feasibility and seeks to improve the objective function in the feasible region, until it eventually reaches the optimum through the new search directions (NSD). The primary objective of the first phase is to assure the feasibility with respect to all the constraints, when important disturbances enter a unit.

Due to a change in the value of the disturbances, constraints will move; as a result, the shape of the feasible region will change. Very often some constraints will move faster than the others, and both the shape and the boundary constraints of the feasible region will change (Figure 6). As the disturbance value changes, g_1 moves into the feasible region, since it moves faster than the other constraints. Operating at the design optimum will not be feasible, because g_1 will be violated. Therefore, before considering any re-optimization, a feasible operating point has to be achieved.

The feasible point algorithm (DeBrosse and Westerberg, 1973) will find such a point by replacing one of the constraints g_2 or g_3 by g_1. This in turn results in two alternative feasible points 1 and 2 (Figure 6). Alternative initial branches will result by either moving along g_3 (i.e., $0' \rightarrow 2$) or moving along g_2 (i.e., $0' \rightarrow 1$). These two different ISD's will have to be accomplished by the existing control structure at 0. Along the path $0' \rightarrow 1$, g_2 will be controlled and the set-point of g_3 will be changed, while along $0' \rightarrow 2$, g_3 will be controlled and set-point of g_2 will be changed.

As soon as disturbance changes are detected through on-line direct or secondary measurements, set-point changes have to be accomplished fast enough to avoid constraint violations during the transient. Monitoring directly the important constraints themselves (by measuring them) will also show how fast they are approached and can be used to decide when to activate ISD's towards the new feasible point. Since some constraints are never to be violated (hard constraints) and some can be allowed to be violated only for a very short time (soft constraints), the set-point changes for the ISD have to be smooth and fast enough.

In the case that no constraint violation results at the current operating point after the disturbances change, there will be no need to find a new feasible point. For example, this would happen if g_1 were not present in Figure 6. In this case, 0 would constitute the feasible point from which the second phase (i.e., search for the optimum) would begin.

Screening Alternative Operational Routes

We will now give guidelines to screen among alternative routes of a sequencing tree to arrive at an acceptable sequence of set-point changes. These guidelines will be most general, while the number of alternatives and the effectiveness of the screening method will depend on the particular unit considered. To develop the screening method, let us examine more closely the characteristics of the nodes of the sequencing tree.

Node Properties

Each node F_{ij} is a steady-state operating point with a set of control objectives to be satisfied. As new constraints are encountered going from one node to another, control objectives will change and control structure modification will be called for. Given a set of control objectives and a set of manipulated variables alternative regulatory control structures can be easily generated at each node F_{ij}. The algorithm to develop feasible alternative control structures as new constraints are encountered at a node is given by Arkun (1979), which is based on the extended structural controllability and observability concepts as formulated by Morari (1977).

Branch and Bound Imbedded Screening Strategy

The strategy makes use of a hierarchy of screening operations.

First Level Screening

i) We start by examining the alternative initial branches of the sequencing tree in terms of *safety and bottlenecking aspects.*

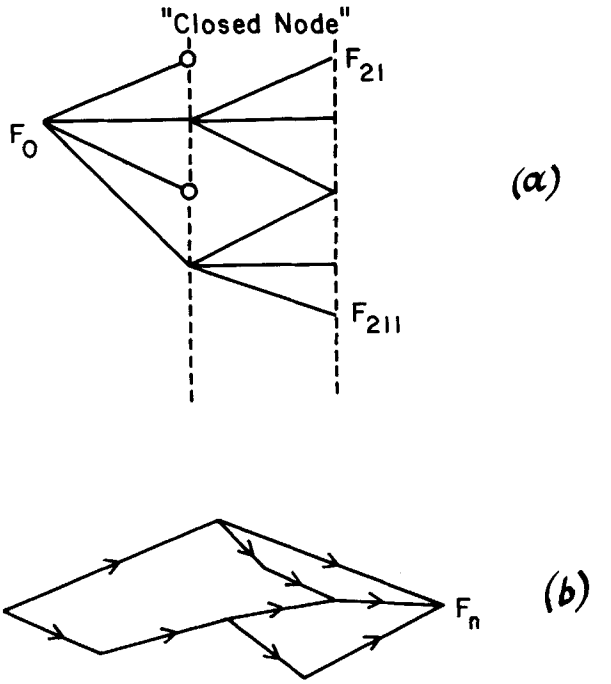

Figure 7. Developing sequencing tree (a) and feasible sequencing routes (b).

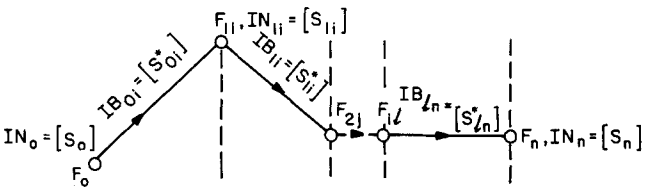

Figure 8. Nodes (IN_{ij}) and branches (IB_{ij}) of an alternative operational route.

Those branches leading to bottlenecks or hazardous situations will not be acceptable. If an initial branch from F_0 to F_{1j} is not acceptable due to safety or bottlenecking, node F_{1j} will be closed, indicating that there will be no operational route going through it (Figure 7a).

ii) After the first branches are analyzed in terms of safety and bottlenecking, we examine the first branch final nodes, F_{1j}'s. Since each F_{1j} represents an operating point with a set of *control objectives*, there should exist at least one feasible control structure to satisfy these objectives. If we cannot generate any feasible control structure at a node F_{1j}, corresponding branch $F_0 \rightarrow F_{1j}$ will be rejected and the node F_{1j} will be "closed."

iii) At the remaining open nodes F_{1j}'s, there will exist *alternative feasible control structures.* Our aim will be to develop effective screening rules which reduce the number of alternatives when they work together and eventually come up with the best control structure at that node. The screening rules start from the simplest and the easiest to implement steady-state considerations and evolve to include dynamic characteristics. The criteria of the screening rules are (Arkun, 1979),

1) Heuristics
2) Steady-state gains
3) Steady-state interactions
4) Time delays
5) Time constants
6) Dynamic interactions
7) Detailed dynamic simulation

The screening eliminates the control structures whose performances lie outside allowable bounds as set by heuristics, steady-state, and dynamic aspects, outlined above. The screen-

ing rules determine the best set of single-input, single-output (S.I.S.O.) control loops. If there is no satisfactory S.I.S.O., multivariable design techniques are tried to interconnect the measurements (i.e., control objectives) with alternative sets of manipulated variables.

If at a node F_{1j} there is no alternative feasible control structure with satisfactory steady-state and dynamic characteristics, that node will be closed and corresponding branch will be rejected. After the screening of the initial branches is complete, we proceed to the second branches emanating from the open nodes of the initial branches (Figure 7a). Branch and bound strategy continues similarly by eliminating the branches that lead to unsafe or bottlenecking situations and/or to the nodes where there is no acceptable control structure. After screening all branches, we arrive at a reduced set of alternative routes between F_0 and the final operating point F_n. (Figure 7b)

We now want to select the best operational route among this reduced set of alternatives which have resulted after the first-level screen. We use a second-level screening which will include the following additional aspects.

Second Level Screening

i) The *number of set-point changes* (i.e., search points) during the optimization should be small. An operational route that requires a large number of set-point changes will not be acceptable, since the process will be over-upset spending most of its time in transient between intermediate steady states before reaching the optimum.

ii) For implementational purposes, the *number of control structure modifications* along a route should be also kept small. Considering single-input, single-output control loops, the selected best S.I.S.O. control structure at node F_{ij} will be represented by the structural pairing matrix S_{ij} as defined by:

$$S_{ij} = \begin{array}{c|cccc} & m_i & m_j & m_k \ldots & m_n \\ \hline c_1 & X & 0 & \ldots\ldots & 0 \\ c_2 & 0 & X & \ldots\ldots & 0 \\ \cdot & \cdot & & & \\ \cdot & \cdot & & 0 & \\ \cdot & \cdot & & & \\ c_n & 0 & \ldots\ldots & & X \end{array}$$

where each diagonal entry, X, indicates the control pair (m_i, c_j) as constructed by the corresponding column and row variables. At each node F_{ij}, current control loops will be classified into the regulatory and servo loops according to the search directions selected at that node. This in turn partitions S_{ij}, and after reordering it we obtain:

$$S_{ij}^* = \begin{bmatrix} \underline{\underline{C}}_{\text{reg}} & & \\ & \underline{\underline{C}}_T & \\ & & \underline{\underline{C}}_R \end{bmatrix}$$

where $\underline{\underline{C}}_{\text{reg}}$ and $\underline{\underline{C}}_T$ are the pairing submatrices for the regulatory loops controlling the regulatory objectives c^p_{reg}, and the tight feasibility constraints c^p_T, respectively. Servo loops corresponding to the released set of constraints are similarly arranged in $\underline{\underline{C}}_R$. Each alternative route can then be described through the structural matrices S_{ij} and S_{ij}^* (Figure 8). The extent of control structure modifications can be easily seen by comparing the structural pairing matrices S_{ij}'s going from one operating point to another along each route. The modifications can be sometimes localized such as repairing of controlled and manipulated variables locally among the (S.I.S.O.) control loops for tight and released constraints. This would result in a change in S_{ij} as:

$$\tilde{S}_{ij} = \begin{bmatrix} \underline{\underline{C}}_{\text{reg}} & & \\ & \tilde{\underline{\underline{C}}}_T & \\ & & \tilde{\underline{\underline{C}}}_R \end{bmatrix}$$

where $\tilde{\underline{\underline{C}}}_T$ and $\tilde{\underline{\underline{C}}}_R$ each contain modified control pairs (m_i, c_j)'s and $\tilde{S}_{ij}$ is the best control structure selected after screening.

Going from a node F_{ij} to F_{lk}, it may not be always possible to rearrange the loops locally within small subsets, but major modification of almost all the previous sets of loops at F_{ij} may be imposed by the control structure selected at F_{lk}. While this is hardly desirable for on-line implementation of optimizing control structures, it might be the only choice for a single-input, single-output control structure that would have satisfactory steady-state and dynamic design characteristics; otherwise, multivariable control could be a better overall alternative.

First of all, control structure modifications arise because different control objectives are encountered along a route. The extent of modifications in the (S.I.S.O.) control loops will depend on the interaction effects introduced by these new controlled variables. Furthermore, the change in the steady-state operating point itself may also introduce interaction effects between the existing loops and require modifications in these loops. The routes which contain too many intermediate operating points with extensive control structure modifications will not be desirable, unless these are the only alternatives available.

iii) The *behavior of the objective function* along alternative routes will constitute the third screening rule. We would like to find operational routes along which the objective function improves continuously towards its optimum value while set-points are changed. The magnitude of the Kuhn-Tucker multiplier can be used to determine the sensitivity of the objective function with respect to the different sets of released constraints (i.e., set-point changes), thus allowing us to determine the objective function's behavior along alternative routes.

Figure 9 demonstrates the behavior of the objective function Φ along two different routes. Along route 1, the objective function improves continuously towards its optimum value Φ^*, whereas along 1′ we have different behavior. Along the first branch of route 1′, the objective function decreases; along the second branch, it improves very fast towards its optimum value Φ^*. Although we achieve improvement in the objective function Φ after each set-point change along 1, it may not be favorable due to unfavorable static or dynamic characteristics, like very slow and sluggish control. On the other hand, route 1′ might be relatively faster, in which case we may have some loss during the set-point changes along the first branch but later we improve

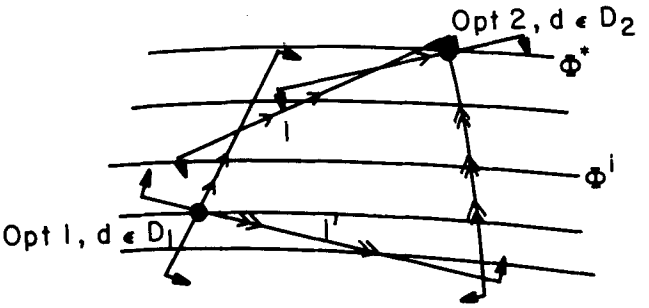

Figure 9. Behavior of objective function along different routes.

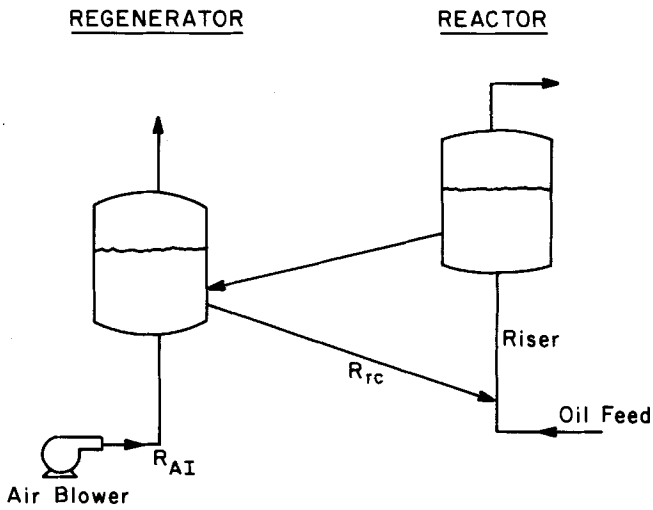

Figure 10. Fluid catalytic cracking unit.

TABLE 1. FCC DESIGN VALUES.

ΔE_{or}	= 63,000 btu/lb · mol (146,200 kJ/kg · mol)	ΔE_{or}	: Activation energy of oxygen reaction
ΔH_{cr}	= 200 btu/lb (464 kJ/kg)	ΔH_{cr}	: Heat of cracking
ΔH_{rg}	= 13,000 Btu/lb (30,160 kJ/kg)	ΔH_{rg}	: Heat of regeneration
ΔH_{fv}	= 75 Btu/lb (174 kJ/kg)	ΔH_{fv}	: Heat of feed vaporization
T_{tf}	= 700°F (370°C)	T_{tf}	: Feed temperature
S_f	= 0.75 Btu/lb · °F (3.14 kJ/kg · °K)	S_f	: Specific heat of feed
T_{ai}	= 250°F(120°C)	T_{ai}	: Air inlet temperature
P_{ra}	= 40 psia (275,600 Pa)	P_{ra}	: Reactor pressure
P_{rg}	= 25 psia (172,250 Pa)	P_{rg}	: Regenerator pressure
F_{tf}	= 100,000 bbl/d	F_{tf}	: Total feed rate
C_1	= 2.0		
C_2	= 5.0 × 10^{-6}		
C_3	= 57.5		
D_{tf}	= 7.3	D_{tf}	: Density of total feed
H_{ra}	= 60 ton	H_{ra}	: Reactor catalyst holdup
H_{rg}	= 200 ton	H_{rg}	: Regenerator catalyst holdup
ΔE_{cc}	= 18,000 Btu/lb · mol (41,760 kJ/kg · mol)	ΔE_{cc}	: Activation energy of catalytic carbon formation
K_{cc}	= 3.73	K_{cc}	: Velocity constant for catalytic carbon formation
K_{cr}	= 358.32	K_{cr}	: Velocity constant for catalytic cracking

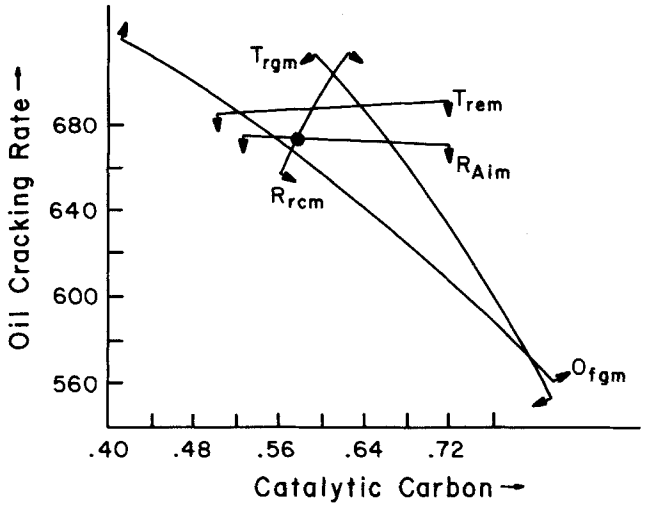

Figure 11. Feasible region for FCC when F_{cf} = 0.

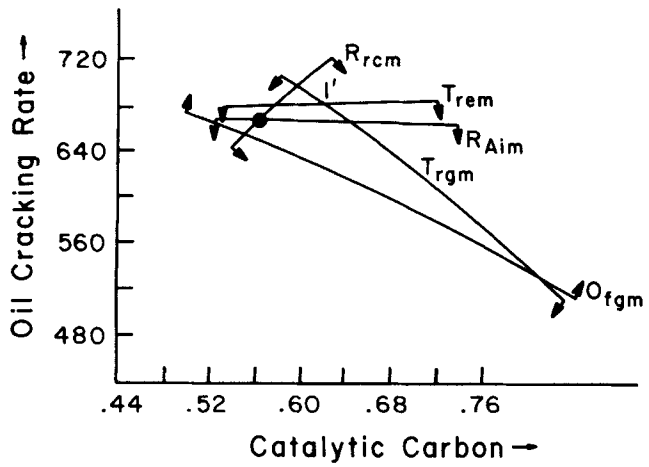

Figure 12. Feasible region for FCC when F_{cf} = 0.01.

economics fast enough to achieve the optimum and operate there for a longer period of time.

As a result, the operational routes which contain branches along which Φ deteriorates will be acceptable only if these are the only remaining alternatives with some other desirable properties such as minimum number of set-point changes, fastness, etc. It is clear that this question requires the solution of a problem of dynamic optimization. In the present work we will deal only with the static aspects leaving the dynamic for a forthcoming publication.

iv) Finally, along an operational route set-point change should be smooth and fast enough. Whereas time constants of the control actions along each branch of a route give a preliminary estimate of fastness of set-point changes, any final choice would be based on *detailed dynamic evaluation* of attractive alternatives left.

NUMERICAL EXAMPLES

We will demonstrate the application of the design methods for steady-state optimizing control to a fluid catalytic cracker and a distillation column.

Steady-State Optimizing Control of a FCC Unit

Fluid Catalytic Cracking (FCC) plants (Figure 10) have been subject to various control and optimization studies, because of the great profit realized through better understanding and optimizing control of these units (Lee and Weekman, 1976; Davis et al., 1974; Webb et al., 1978). Various process constraints determine the conversion capacity of these units which requires close tracking of process constraints in the presence of important disturbances to load the units against optimum set of constraints.

The process models used for this study were those given by Kurihara (1967) which are steady-state material and energy balances around the reactor and the regenerator.

The important constraints considered were those on the reactor and the regenerator temperatures, upper limits on the catalyst recirculation rate and on the air supply to the regenerator, and the oxygen content in flue gas:

$T_{re} \leq$ 930°F (500°C)
Reactor Temperature

$T_{rg} \leq$ 1200°F (650°C)
Regenerator Temperature

$R_{rc} \leq$ 60 tons/min
Catalyst Recirculation Rate

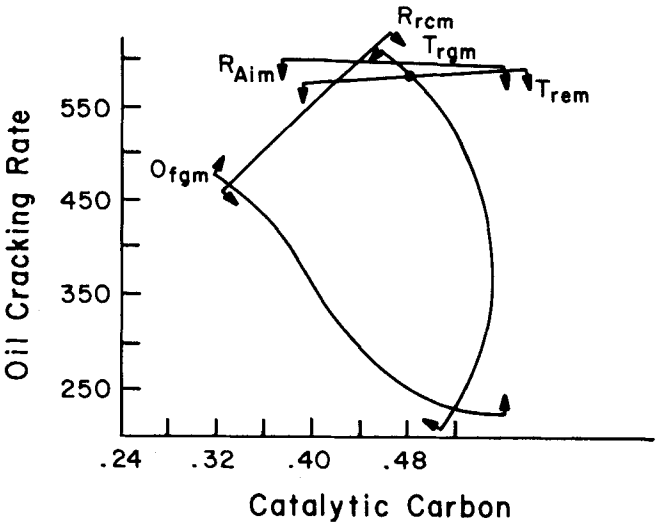

Figure 13. Feasible region for FCC when F_{cf} = 0.1.

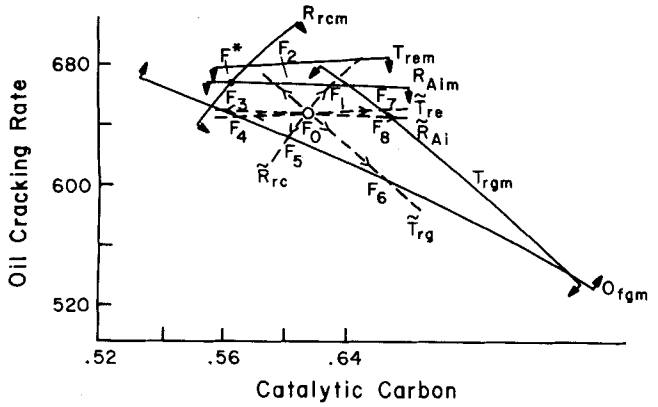

Figure 14. Alternative initial branches from a feasible point to new optimum when F_{cf} decreases from 0.1 to 0.01.

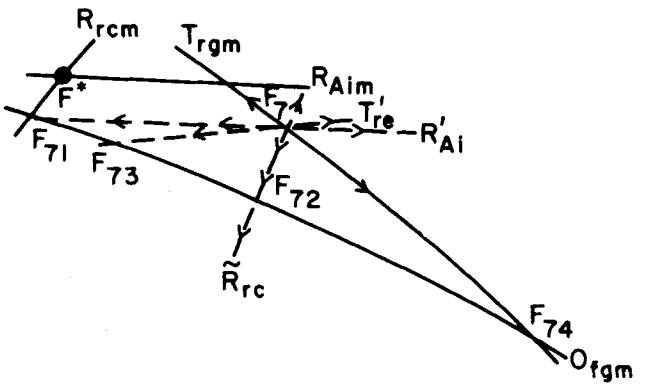

Figure 15. Alternative branches emanating from F_7.

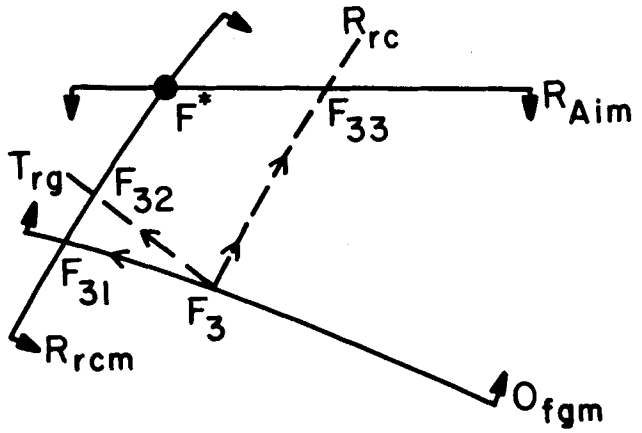

Figure 16. Alternative branches emanating from F_3.

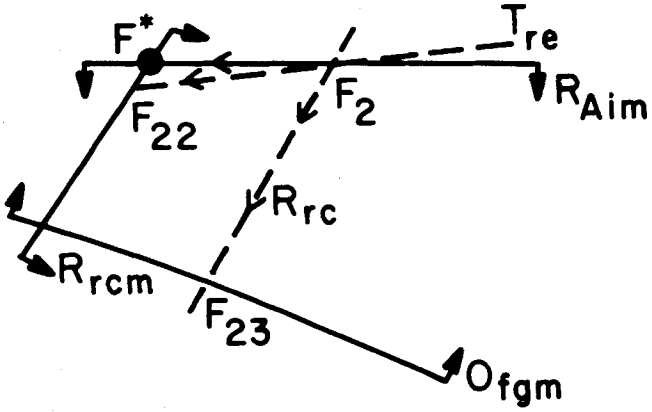

Figure 17. Alternative branches emanating from F_2.

$O_{FG} \leq 0.2$ mol%
Oxygen in the Flue Gas

$R_{Ai} \leq 400{,}000$ lb/h
(180,000 kg/h)
Air Blower Capacity

These constraints were the most important ones which result due to safety and equipment limits in industrial practice.

Temperatures are constrained by the metallurgy of the units, O_{FG} must be maintained at safe values to avoid afterburning of CO to CO_2 with excessive temperature increase in the flue gas. Air flowrate and the catalyst recirculation rates are limited by the air blower capacity and the catalyst slide valve. Typical values for the design parameters and operating variables are given in Table 1.

The total degrees of freedom for FCC were found to be 2 for specified feed temperature, flowrate, reactor, and regenerator hold-ups. Gas oil cracking rate R_{oc} could then be easily plotted against the catalytic carbon content on spent catalyst, C_{cat} along each constraint to give the feasible region as shown in Figure 11. Any operating point in the feasible region uniquely determines all the process variables and with that the objective function Φ. The assumed objective function was the conversion c_{tf} of the feed where gas and gasoline were taken to be the valuable products of the gas oil cracking.

Since $c_{tf} = R_{oc}/1.75\, D_{tf} R_{tf}$ (Kurihara, 1967), *where* D_{tf} and R_{tf} are the specified density and the flowrate of the feed, one can easily locate where maximum conversion lies in the feasible region for various disturbances as we shall now examine.

Effect of F_{cf} of Feed on FCC Operation

The principal disturbance which affects the optimal operation is the coke formation factor F_{cf} of the feed which will vary from one feedstock to another (Kurihara, Gould, and Evans, 1970; Pohlenz, 1963). Figures 11 through 13 show how the feasible regions and optimal operating point moves for three different values of disturbances. As the feed quality gets worse (i.e., F_{cf} increases), the optimum conversion decreases and it moves to the intersection of different constraints.

Effects of Disturbances on the Optimizing Control Strategy

We will now see how the optimizing control strategy changes as an FCC becomes subject to different feedstocks. For a heavier feed with $F_{cf} = 0.1$, the optimum operating point is at the intersection of the reactor and regenerator upper temperatures T_{rem}, T_{rgm} with conversion $c_{tf} = 0.4579$. To maintain this maximum conversion, both active temperatures are controlled on their upper limits.

Primary controlled variables c^p are one active constraint for each process unit, i.e., reactor and regenerator,

$$c^p_1 = T_{re} \quad c^p_{1d} = T_{rem}$$
$$; \qquad \text{— Current Optimum Set-Points}$$
$$c^p_2 = T_{rg} \quad c^p_{2d} = T_{rgm}$$

Once the controlled variables are identified, we identify manipulated variables within each unit to constitute the local optimizing control loops for the reactor and the regenerator. The available manipulated control variables for the regenerator and the reactor are R_{Ai} and R_{rc}, respectively. R_{Ai} is manipulated to

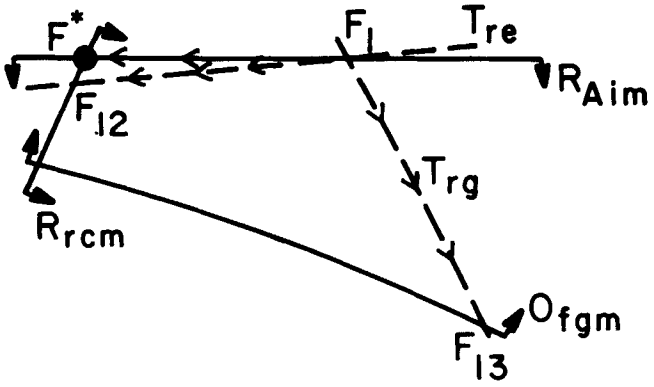

Figure 18. Alternative branches emanating from F_1.

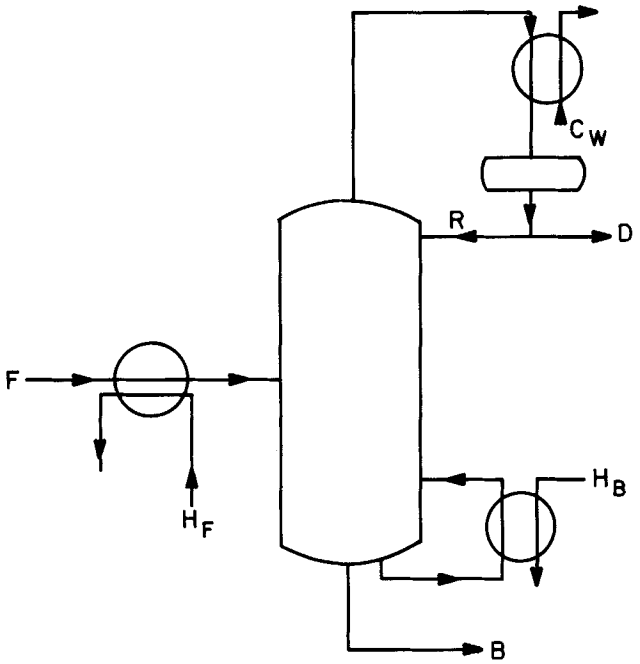

Figure 20. Distillation column system.

control T_{rg}; R_{rc} is manipulated to control T_{re}. Current control loops at optimum are:

$$1)\ (R_{rc},\ T_{re}), \qquad 2)\ (R_{Ai},\ T_{rg}).$$

This control structure is similar to the conventional control system (Lee and Weekman, 1976) except that since $O_{fg} << O_{fg,max}$ at the optimum, it is not directly controlled but is kept at safe levels through the control of T_{rg} instead. When a lighter feed (i.e., $F_{cf} = 0.01$) is processed, the optimum moves to the intersection of R_{rc} and R_{Ai} as shown in Figure 12. Since the feed quality improves, the optimum conversion increases (c_{tf} = 0.5214), and FCC has to be controlled at the new set of constraints to make use of this additional capacity. We will now generate alternative operational routes towards this new optimum.

Finding a Feasible Point

After F_{cf} changes from 0.1 to 0.01, the control of T_{re} and T_{rg} on their upper bounds will not be feasible due to air blower capacity limits as shown by point 1′ in Figure 12. Hence, a feasible point F_0 is found for $F_{cf} = 0.01$ by setting the manipulated variables at their last values before F_{cf} has changed, Figure 14.

At F_0:

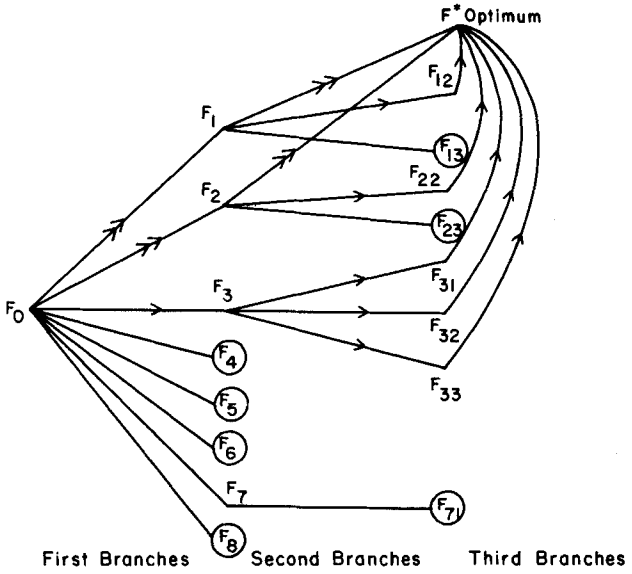

Figure 19. Tree of alternative and acceptable operational routes (0 = terminated nodes).

$$R_{rc} = \tilde{R}_{rc} = 53.52 \qquad T_{re} = \tilde{T}_{re} < 930(500°C)$$

;

$$R_{Ai} = \tilde{R}_{Ai} = \begin{matrix} 391{,}400 \\ (176{,}700 \end{matrix} \text{ kg/h}) \qquad T_{rg} = \tilde{T}_{rg} < 1200(650°C)$$

Since the feed is lighter, the coke production rate decreases which results at lower regenerator and reactor temperatures. Setting manipulated variables at above values, we move into the feasible point F_0 from which alternative routes will branch out along the current constraint envelope.

Generation of Alternative Paths at F_0

Movement along the four current constraints at F_0 in either direction until a new constraint is encountered generates eight possible initial branches to start the search towards the new optimum F^* as shown in Figure 14. Let us examine these initial alternative branches in terms of their operational objectives.

$F_0 \rightarrow F_1$: Movement is along $R_{rc} = \tilde{R}_{rc}$; set-point of T_{rg} is increased by increasing R_{Ai}. At F_1, air supply is at maximum limit beyond which T_{rg} cannot be increased.

$F_0 \rightarrow F_2$: Movement is along $T_{rg} = \tilde{T}_{rg}$, *where* T_{re} set-point is continuously increased by increasing R_{rc}. Assuming single-input, single-output loops:

Servo loop: $(T_{re} - R_{rc})$
Regulatory loop: $(T_{rg} - R_{Ai})$.

At F_2, R_{Ai} constraint is encountered beyond which T_{re} set-point cannot be increased.

TABLE 2. FEED DESIGN SPECIFICATIONS FOR DEPROPANIZER.

Components	lb·mol/h	(kg·mol/h)
Propane	106.4851	(48.35)
I-Butane	50.6496	(22.99)
N-Butane	45.0408	(20.45)
I-Pentane	7.5	(3.40)
N-Pentane	2.5	(1.14)
Propylene	4.8588	(2.21)
Cis-2-Butene	1.1427	(0.52)
Trans-2-Butene	0.8571	(0.39)
I-Butene	2.86	(1.30)
Tr-2-Pentene	0.2856	(0.13)
Heptene	38.7611	(17.60)
TOTAL	260.9409	(118.48)

$F_0 \rightarrow F_3$: Search is along $R_{Ai} = \tilde{R}_{Ai}$, and T_{re} set-point is changed by manipulating R_{rc} until O_{FG} constraint is encountered at F_3. This path demonstrates how set-point changes in one unit (reactor) may violate the constraints in the next interconnected unit (regenerator). Also, along this path conversion increases very little compared to the path $F_0 \rightarrow F_2$. The real disadvantage of this path over the first one is in terms of safety and additional control effort required. At F_3, O_{fg} constraint becomes active violation of which may lead to afterburning and hazardous temperature rises in the flue gas, unless it is closely monitored through gas analyzers and controlled. Control structure modification will be necessary at F_3, *where* R_{Ai} previously controlling T_{rg} will now be used to control O_{fg}.

New control structure at F_3:

$$(O_{fg} - R_{Ai})$$

$$(T_{re} - R_{rc})$$

which interestingly corresponds to the conventional control scheme (Lee and Weekman, 1976).

Paths $F_0 \rightarrow F_4$, $F_0 \rightarrow F_5$, $F_0 \rightarrow F_6$ will not be acceptable first branches, since they all end on the O_{fg} constraint as the path $F_0 \rightarrow F_3$ does. Furthermore, they lead to a decrease in the objective function which make $F_0 \rightarrow F_3$ favorable over all these branches.

$F_0 \rightarrow F_7$: The reactor temperature is regulated at set-point $\tilde{T}_{re}$ and the regenerator temperature is increased by increasing the air supply.

$$\text{Servo loop:} \qquad (T_{rg} - R_{Ai})$$

$$\text{Regulatory loop:} \ (T_{re} - R_{rc})$$

$F_0 \rightarrow F_8$: Movement is along $R_{Ai} = \tilde{R}_{Ai}$; set-point of T_{re} is changed by manipulating R_{rc} until the regenerator temperature constraint T_{rgm} is encountered. This branch will not be acceptable, since it leads to a decrease in the objective function.

We, therefore, have four initial alternative branches after eliminating $F_0 \rightarrow F_4$, $F_0 \rightarrow F_5$, $F_0 \rightarrow F_6$, $F_0 \rightarrow F_8$.

Generation of Second Branches at Each Feasible Node

Starting from the nodes F_1, F_2, F_3, and F_7 where initial branches have terminated, second branches will be developed.

Branches Emanating from F_7. Alternative routes will exist by moving along the current constraints at F_7 as depicted in Figure 15.

Movement along R'_{rc} and T'_{re} in increasing objective function direction is not feasible, since T_{rgm} is violated. Moving along R_{Ai} in the feasible region, O_{fg} constraint is met at F_{71} with an improvement in conversion. Moving along T_{rgm} to increase the objective function ends at a structurally infeasible node (R_{Aim}, T_{rgm}), where we have two control objectives (i.e., two active constraints) with one manipulated variable R_{Aim}. This branch and every route going through this node will not be acceptable. After screening also the other branches along which the conversion decreases (i.e., $F_7 \rightarrow F_{72}$, $F_7 \rightarrow F_{73}$, $F_7 \rightarrow F_{74}$), the only acceptable branch is $F_7 \rightarrow F_{71}$.

Branches from F_3. After eliminating the branches that move out of the feasible region and away from the optimum, we will have three branches towards F^* as shown in Figure 16. These branches are:

1) $F_3 \rightarrow F_{31}$ along O_{fgm} constraint
2) $F_3 \rightarrow F_{32}$ along T_{rg} = constant
3) $F_3 \rightarrow F_{33}$ along R_{rc} = constant

Branches from F_2. The alternative branches are shown in Figure 17. These alternatives are as follows:

1) $F_2 \rightarrow F_{21} \equiv F^*_{opt}$ along R_{Aim} constraint by changing T_{re} set-point

2) $F_2 \rightarrow F_{22}$ along T_{re} = constant until R_{rcm} is encountered

3) $F_2 \rightarrow F_{23}$ along R_{rc} = constant until O_{fgm} is encountered

Branch 3) is not acceptable because it is a path leading away from the optimum, to the nodes on O_{fgm} constraint similar to the ones generated and eliminated before.

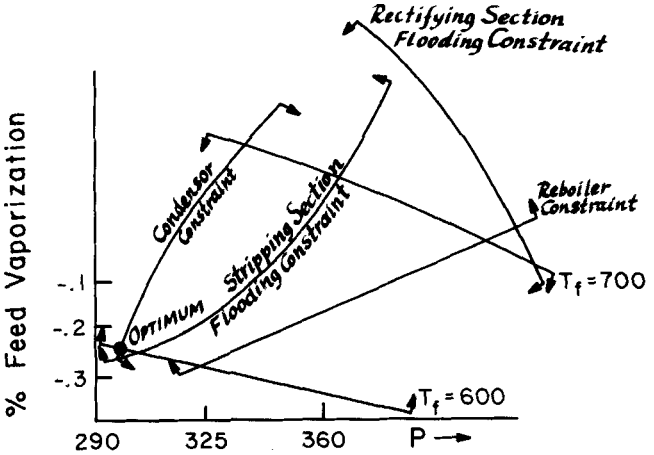

Figure 21. Feasible operating region for depropanizer at optimum design conditions.

Branches from F_1. Figure 18 shows the alternative branches from F_1. The branches are given by:

1) $F_1 \rightarrow F_{11} \equiv F^*_{opt}$
along R_{Aim}
2) $F_1 \rightarrow F_{12}$
along T_{re} = constant until R_{rcm} is encountered
3) $F_1 \rightarrow F_{13}$
along T_{rg} = constant until O_{fgm} is encountered

Branch 3) is eliminated by the same reasoning applied to the branch $F_2 \rightarrow F_{23}$.

Generation of Third Branches

We have six feasible nodes from which new operational routes will emerge, F_{12}, F_{22}, F_{31}, F_{32}, F_{33}, F_{71}.

From F_{71}. The third branches emanating from F_{71} are similar to the second branches (i.e., F_{31}, F_{32}, F_{33}) which have been previously developed at F_3. Therefore, $F_0 \rightarrow F_3 \rightarrow F_{31} \rightarrow F^*_{opt}$ will be favored over $F_0 \rightarrow F_7 \rightarrow F_{71} \rightarrow - - \rightarrow F^*_{opt}$ because of the smaller number of set-point changes. This will reduce the initial branches to a total of three:

$$F_0 \rightarrow F_1, \ F_0 \rightarrow F_2, \ F_0 \rightarrow F_3$$

From F_{31}.

$$F_{31} \rightarrow F^*_{opt} \text{ along } R_{rcm}$$

From F_{32}.

$$F_{32} \rightarrow F^*_{opt} \text{ along } R_{rcm}$$

From F_{33}.

TABLE 3. OPTIMUM DESIGN CONDITIONS FOR DEPROPANIZER.

Pressure, P	= 297 psia (2,046 kPa)
% Feed Vaporization	= −28.83%
Reflux Ratio, R	= 2.1541
Bottoms, B	= 153.97 lb·mol/h (69.90 kg·mol/h)
Distillate, D	= 106.96 lb·mol/h (48.56 kg·mol/h)
Feed Temperature, T_f	= 600°R(60°C)
Reboiler Steam Usage, H_B	= 4,506 lb/h (2,048 kg/h)
Cooling Water Usage, C_w	= 8,824.53 gal/h (2,322 L/h)
Flooding in Rectifying Section	= 50%
Flooding in Stripping Section	= 90%
ΦUtilities	= 78,364 $/yr

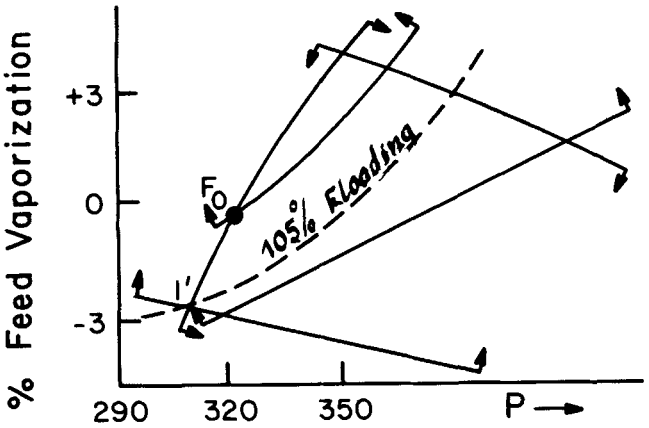

Figure 22. Feasible region for distillation column after feed flowrate increased at F = 275 lb·mol/h (124 kg·mol/h).

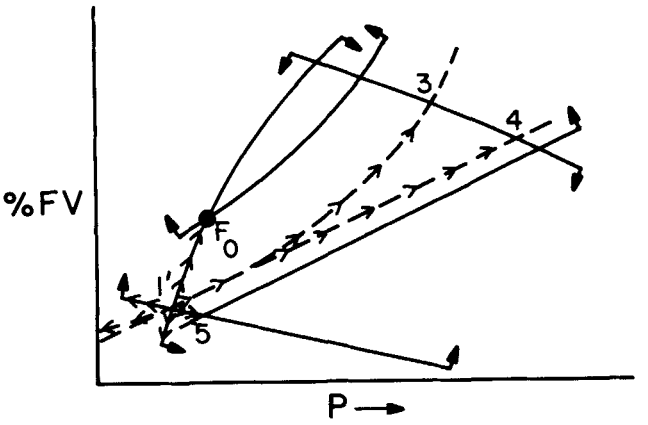

Figure 23. Alternative branches towards new optimum after feed flowrate increased (F = 275).

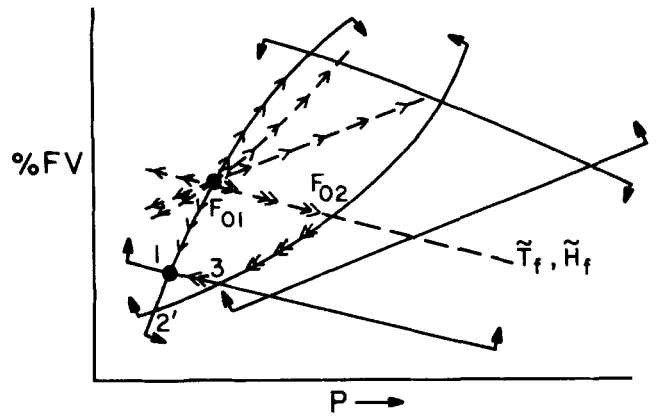

Figure 24. Alternative branches towards new optimum after feed flowrate decreased.

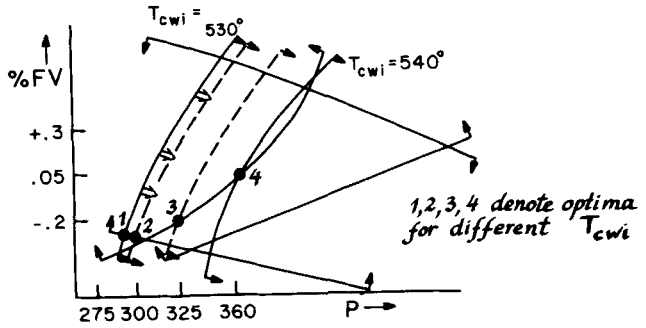

Figure 25. Movement of condenser constraint with inlet cooling water temperature.

$$F_{33} \rightarrow F^*_{opt} \text{ along } R_{Aim}$$

From F_{12}.

$$F_{12} \rightarrow F^*_{opt} \text{ along } R_{rcm}$$

From F_{22}.

$$F_{22} \rightarrow F^*_{opt} \text{ along } R_{rcm}$$

As a result, we have the following alternative sequences to be further screened:

1) $F_0 \rightarrow F_1 \rightarrow F^*_{opt}$

2) $F_0 \rightarrow F_1 \rightarrow F_{12} \rightarrow F^*_{opt}$

3) $F_0 \rightarrow F_2 \rightarrow F^*_{opt}$

4) $F_0 \rightarrow F_2 \rightarrow F_{22} \rightarrow F^*_{opt}$

5) $F_0 \rightarrow F_3 \rightarrow F^*_{opt}$

6) $F_0 \rightarrow F_3 \rightarrow F_{32} \rightarrow F^*_{opt}$

7) $F_0 \rightarrow F_3 \rightarrow F_{33} \rightarrow F^*_{opt}$

The tree of alternative operational routes is shown in Figure 19. The paths going through the node F_3 along the O_{fgm} constraint (routes 5, 6, 7) will be disfavored due to encountering critical flue gas constraint and control structure modification hence required as described before. Furthermore, 1) and 3) are favored over 2) and 4) because of their fastness and less number of set-point changes required. Consequently, we arrive at the two acceptable sequences:

1) $F_0 \rightarrow F_1 \rightarrow F^*_{opt}$

2) $F_0 \rightarrow F_2 \rightarrow F^*_{opt}$

and let us identify the optimizing strategy along each path in detail,

1. As FCC is subject to lighter feedstock, the catalyst circulation rate R_{rc} is kept constant at its current value R_{rc} and the set-point of the regenerator temperature is increased by increasing R_{Ai}. At $R_{Ai} = R_{Aim}$, air supply is kept maximum and the set-point of the reactor temperature T_{re} is increased by increasing R_{rc}; until one arrives at the new optimum conversion at $R_{rc} = R_{rcm}$, $R_{Ai} = R_{Aim}$. The search is first initiated by the local optimizer of the regenerator unit, *where* $(T_{rg} - R_{Ai})$ constitutes the servo loop; then, it is taken over by the reactor unit local optimizer, *where* $(T_{re} - R_{rc})$ constitutes the servo loop.

2) Starting from F_0, T_{re} set-point is increased by increasing R_{rc} and at the same time regulating T_{rg} at its current value T_{rg} by manipulating R_{Ai}. This defines one servo loop in the reactor and one regulatory loop in the regenerator. At $R_{Ai} = R_{Ai\max}$, air supply is kept at maximum and T_{re} set-point is increased by manipulating R_{rc} until the optimum is achieved.

Steady-State Optimizing Control of a Distillation Column

The second example on single units considers a depropanizer as shown in Figure 20. The design specifications for the feed are given in Table 2. The process simulator CHESS (Motard et al. 1968), together with the costing subroutines given by the system PROPS (Gaines and Gaddy 1974) were employed during the simulation of the distillation column.

Optimization Problem

The objective function is the maximization of the profit:

Max {Φ = Product Revenue − Raw Material Cost − Utilities}
subject to the column constraints.

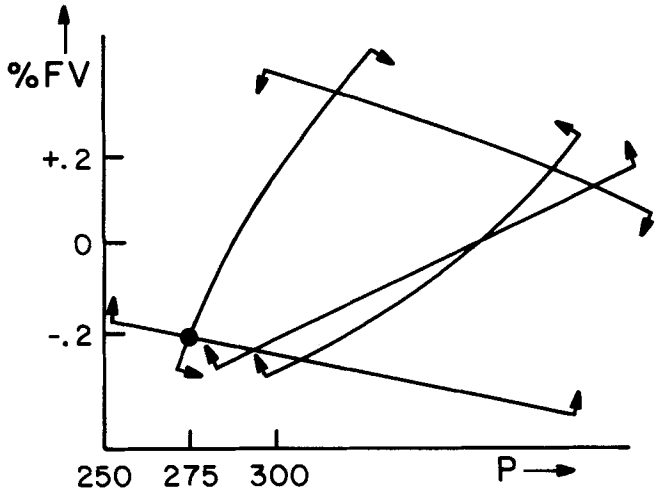

Figure 26. Feasible region for distillation column after ratio of propane/olefins in feed decreased.

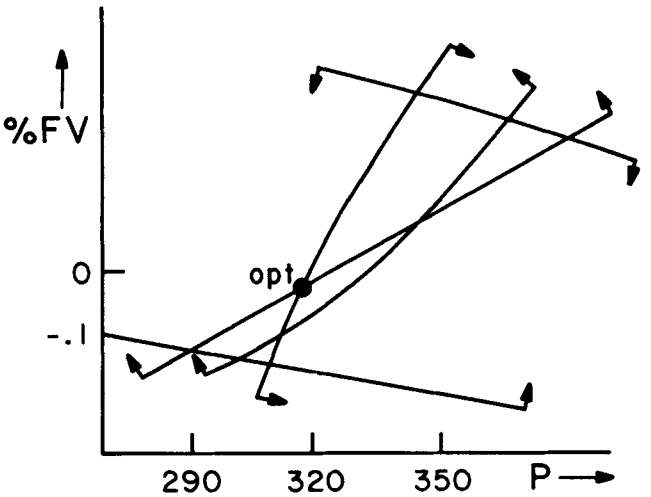

Figure 27. Effect of an increase in propane to butanes ratio in feed on location of operating optimum for depropanizer.

For specified feed flowrate, composition and recoveries, distillate and bottoms product rates are fixed; optimization problem becomes the minimization of utilities.

Column Constraints

Optimization will be subject to the following operational constraints:

Flooding constraints in the rectifying and stripping sections of the column: percent flooding during the operation should not exceed 95% which is the maximum allowable column capacity.

Reboiler Constraint. Max steam temperature available is $T_{stm,reb} \leq 910°R(235°C)$.

Condensor Constraint. Minimum increase in the cooling water temperature is $\Delta T_{cw} \geq 25°F(14°C)$.

Feed Temperature Constraints. The temperature of the feed at the exit of the preheater is constrained from below and above due to the feed preheater design constraints. Maximum temperature to which feed can be preheated and the minimum temperature (i.e., when the heating fluid valve is closed) are $600°R(60°C) \leq T_f \leq 700°R(116°C)$.

The feasible operating envelope is shown in Figure 21. The percent feed vaporization and the column pressure were taken as the free variables to construct the feasible region. Any operating point in this region uniquely determines the values of the column variables and with that the objective function Φ. The design optimum is at the intersection of the condensor and the feed temperature constraints. At this design optimum, the values of the column variables are given on Table 3. The optimum is at the minimum column pressure allowable. This is usually the case for the columns where the separation is easier at lower pressures (Maarleveld, Rijnsdorp; 1970).

Optimizing Control Structure

Since the feed temperature is at its lower bound, $T_f = 600(60°C)$, at the design optimum, the first optimizing control objective is to keep the preheater valve closed: $m_{1D} = H_F = 0$.

The second optimizing control objective is to keep the condensor constraint active which will denote the primary controlled variable as: $c^p_1 = T_{cwo}$, *where* T_{cwo} is cooling water outlet temperature.

Manipulated variable is $m_{2D} = C_w$ (cooling water flowrate).

Note that the column pressure is not under direct control. It is indirectly controlled by manipulating the cooling water flowrate to control one of the active constraints, i.e., the cooling water temperature rise on its bound, $\Delta T_{cw} = 25°(14°C)$. The current optimizing control structure removes two degrees of freedom, i.e., C_w, H_F; while other manipulated variables such as R, B, D are involved in various regulatory loops to maintain the material balance control.

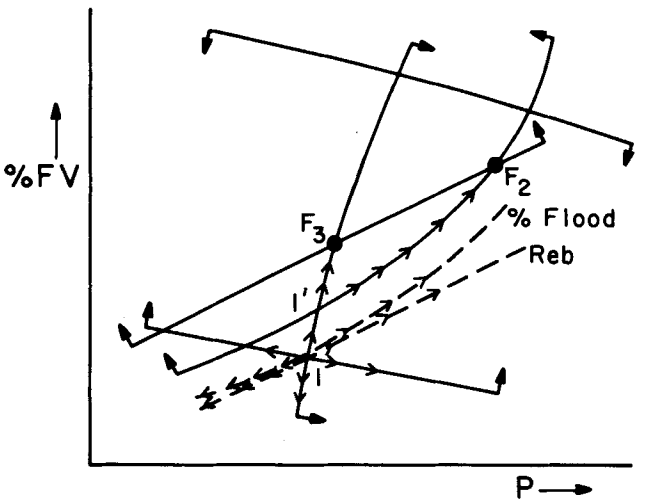

Figure 28. Alternative branches towards a feasible point after a feed composition change for depropanizer.

Effect of Disturbances on Optimal Column Operation

We will now analyze the economic impacts of important disturbances such as feed flowrate, feed composition, and cooling water temperature.

Feed Flowrate Disturbance. Consider that the flowrate increases to 275 lb · mol/h (124 kg · mol/h). The new optimum is shown in Figure 22. At the new optimum, a new constraint becomes active, i.e., the stripping section trays are loaded just to the allowable capacity, 95% flooding. The preheater constraint is no more active, the feed enters the column at 660°R(94°C). We will now generate alternative routes to go from one optimum to another.

After flowrate, F, increases, the current optimizing control structure (i.e., condenser and preheater constraints are kept tight) will not constitute a *feasible operating point.* This is because flooding will occur on the stripping section trays (i.e., % flooding—105%) at this operating point 1', Figure 22. Therefore, a feasible point F_0 is found through replacing the preheater constraint by the flooding constraint, Figure 22.

Emanating from 1' there are eight *alternative paths.* These result from moving in two possible directions along the four constraints at their current values at 1' after flowrate has changed, Figure 23. The four branches that move away from the feasible region are automatically screened. The paths 1 → 3 (along Reboiler constraint), 1 → 4 (along the flooding con-

straint), $1 \rightarrow 5$ (along the preheater constraint) are also eliminated, since the column moves away from the optimum, and it also does not recover from flooding. Hence, $1' \rightarrow F_0$ is the only favorable alternative and let us examine the optimizing control steps taking along this route.

Movement is along the condenser constraint which is accomplished by partially opening the preheater valve to increase the feed temperature. Condenser constraint is kept tight by controlling the cooling water temperature rise at its current set-point by manipulating the cooling water flowrate. Movement along $1' \rightarrow F_0$ will uniquely determine the values of all the other column variables: pressure will increase and reboiler steam supply will decrease. Opening the preheater valve, decreasing the reboiler supply will unload the trays in the stripping section and increase the load on the rectifying section trays.

At the feasible point F_0, the new active flooding constraint constitutes the new control objective. The pressure drop over the stripping section can be measured to infer the flooding conditions. New primary controlled variable $c^p_1 = \Delta P_s$. To control ΔP_S and hence the tray load, the steam flow in the reboiler, H_B, is manipulated. H_B affects the vapor flow in the column very fast and quite often is used for ΔP control, (Rademaker et al. 1975). Hence, the optimizing constraint control structure at F_0 is given by the control loops: $(H_B, \Delta P_s)$, (C_w, T_{cwo}).

Since F_0 is also the optimum, the search is terminated after ISD elapses and the above control structure modification is accomplished. For further increase in F, the feasible region will shrink but the optimum will stay at the intersection of the condenser and flooding constraints. Hence, control of the same constraints on their bounds will guarantee optimality for reasonable flowrate changes.

Now let us examine the reverse case when F decreases from 275(124) to 260 lb·mol/h (117.5 kg · mol/h) and generate alternative routes. The feasible region after the flowrate has decreased is shown in Figure 24. When flowrate decreases, the current control policy of keeping the flooding and the condenser constraints tight will lead to the infeasible point 2'. Hence, a new feasible point is to be found.

Alternative feasible points will result depending on the different constraints to be released. If the flooding constraint is not kept tight, a feasible point F_{01} can be achieved when the condenser constraint is controlled and the manipulated variable H_F is set at its last value $\bar{H}_F$ before the flowrate decreases Figure 24. As a second feasible point F_{02}, condenser constraint could be released and the flooding constraint is controlled while keeping H_F at its last value $\bar{H}_F$ again.

F_{01} will be automatically achieved if C_w is manipulated to keep the condenser constraint tight, if H_F is unchanged (i.e., $H_F = \bar{H}_F$) and if the reboiler steam supply H_B is adjusted to its new value at F_{01}. The second feasible point F_{02} can be achieved by keeping $H_F = \bar{H}_F$ and changing the set-point for the condenser constraint control loop along $F_{01} \rightarrow F_{02}$.

The search will continue either from F_{01} or F_{02} towards the optimum point 1. Note that $F_{01} \rightarrow F_{02}$ constitutes one of the eight alternative branches from F_{01} to the optimum. The route $F_{01} \rightarrow 1$ directly takes the column to the optimum. Along this path, condenser constraint is controlled, H_F is continuously decreased and H_B is increased until the preheater valve is closed at 1, i.e., $H_F = 0$. F_{02} as an alternative feasible point or as an intermediate steady-state operating point is not selected because: 1) the objective function increases along $F_{01} \rightarrow F_{02}$ and 2) we have a large number of set-point changes along the route passing through F_{02} ($F_{01} \rightarrow F_{02} \rightarrow 3 \rightarrow 1$) to arrive at the optimum.

Cooling Water Temperature Disturbance. The design optimum for the inlet cooling water temperature T_{cwi} = 530°R(21°C) is shown in Figure 20. For $T_{cwi} > 530$°R(21°C), the condenser constraint moves as shown in Figure 25, where it becomes active at higher pressures. The optimum first moves along $H_f = 0$, i.e., $T_f = 600$°R(60°C) for a few degrees change and control of the condenser constraint and keeping preheater valve closed leads to the optimum. The optimizing control actions to move to the new operating points will be the same as discussed for feed flowrate disturbance.

Feed Composition Disturbances. We considered two types of feed composition disturbances: 1) d_1 (propane to olefin ratio) and 2) d_2 (propane to butanes ratio).

For a decrease in d_1, the feasible region is shown in Figure 26. Both top and bottom temperatures increase and, reboiler and condenser constraints are encountered at lower pressures. This explains the direction of movements of constraints. For a wide range of disturbances, the optimum is at the intersection of the condenser and preheater constraints, and control of these constraints leads to the optimum operation.

For an increase in d_2, the feasible region is shown in Figure 27. The optimum is at the intersection of the reboiler and condenser constraints. After the feed composition changes, control of the condenser constraint and keeping the preheater valve closed will result in an infeasible operation policy since flooding and reboiler constraints will be violated, Figure 27. H_f will have to be partially opened to recover feasibility with respect to these constraints.

Alternative branches towards the feasible points F_2 and F_3 are shown in Figure 28. Movement along the condenser constraint $(1 \rightarrow F_3)$ requires the manipulation of C_w and at the same time opening of the preheater valve. This control action first unloads the stripping section trays, and the column will be feasible with respect to the flooding constraint at 1'. But, it is still infeasible with respect to the reboiler constraint. To recover feasible operation, the preheater valve has to be further opened along $1' \rightarrow F_3$. At F_3, the feasible point is reached where the condenser and reboiler constraints are active.

Note that $1' \rightarrow F_2$ constitutes an alternative path to a feasible point where one moves along the flooding constraint by controlling ΔP_s. This was automatically eliminated since the objective function increases, and it is a slower path with greater number of set-point changes.

At F_3, there is no need for new search directions since it is also the optimum. Condenser constraint is controlled, the reboiler steam is at its highest available pressure.

ACKNOWLEDGMENT

The financial support of the National Science Foundation through the Grant ENG 75-11165-A01 is gratefully acknowledged.

NOTATION

c^p = primary controlled variable vector composed of active design constraints (c^p_{opt}) and regulatory control objectives (c^p_{reg})
c^s = vector of secondary controlled variables
c^p_d = vector of set-points for the primary controlled variables
c^p_R = vector of released constraints
c^p_T = vector of tight constraints
c'^p_{opt} = set of previously active design constraints at X^* that remain active at X°
$\tilde{c}^p_{\text{opt}}$ = set of previously active design constraints at X^* that become inactive at X°
$\bar{c}^p_R$ = vector of controlled variables deleted from c^p_R when new constraints ($\bar{g}_{IA}$) become active
$\bar{c}^p_R$ = new set of released constraints after $\bar{c}^p_R$ is excluded from c^p_R
d = vector of disturbances
d' = new values for disturbances after they deviate from their design values
d^* = design values for disturbances
f = vector of lumped active constraints
g' = system's state functions
g'' = process design constraint functions
g_{IA} = vector of inactive design constraints

g'_{IA} = set of previously inactive design constraints at X^* that become active at the feasible point X° after disturbances change (i.e., $d = d'$)
$\tilde{g}_{IA}$ = set of previously inactive design constraints at X^* that remain inactive at X° after disturbances change
$\bar{g}_{IA}$ = vector of inequality design constraints which become active at a search point
L = Lagrangian function
m = vector of manipulated variables
$\tilde{m}$ = vector of extrafree manipulated variables
m_D = vector of manipulated variables controlling primary controlled variables
r = regulatory control functions
x = vector of states
$\bar{x}$ = vector of variables composed of x, d, and m_D
$\tilde{x}$ = vector of variables composed of x and m_0.
X° = a feasible operating point
X^* = design optimum

Greek Letters

β = constrained sensitivity of Φ with respect to $\tilde{m}$ at X°
λ = vector of Lagrange multipliers for equality constraints $f(\bar{x}, \tilde{m}) = 0$
λ_A = vector of Kuhn-Tucker multipliers for active design constraints
λ_{IA} = vector of Kuhn-Tucker multipliers for inactive design constraints
Φ = objective function
∇ = gradient operator

LITERATURE CITED

Arkun, Y., "Design of Steady-State Optimizing Control Structures for Chemical Processes," Ph.D. Thesis, Univ. of Minnesota (March, 1979).

Barkelew, C. H., "Modern Process Control—State of the Art in Petroleum Refining," *AIChE Symp.* Ser. 159, **72** (1976).

Baxley R. A., "Local Optimizing Control for Distillation," *Instrumentation Tech.*, 75 (Oct., 1969).

Buckley P. S., *Techniques of Process Control*, J. Wiley & Sons, Inc. (1964).

Davis, T. A., D. E. Griffin, and P. U. Webb, "Cat Cracker Optimization and Control," *Chem. Eng. Prog.*, **70**, No. 11, 53 (Nov., 1974).

DeBrosse C. J., and A. W. Westerberg, "A Feasible-Point Algorithm for Structured Design Systems in Chemical Engineering," *AIChE J.*, **19**, No. 2, 251 (1973a).

Douglas, J. M., "Preliminary Process Design Part III, Quick Estimates of Control Economics," *AIChE Annual Meeting*, New York (1977).

Duyfjes, G., and P. M. E. M. Van Der Grinten, "Application of a Mathematical Model for the Control and Optimization of a Distillation Plant," *Automatica*, **9**, 537 (1973).

Ellingsen, W. R., "Implementation of Advanced Control Systems, *AIChE Symp.* Ser. 159, **72** (1976).

Findeisen, W., "Lectures on Hierarchical Control Systems," Univ. of Minnesota (1976).

Gaines, L. D., and J. L. Gaddy, "Univ. of Missouri-Rolla PROPS Users' Guide," Rolla, MO (1974).

Gould, L. A., L. B. Evans, and H. Kurihara, "Optimal Control of Fluid Catalytic Cracking Processes," *Automatica*, **6**, 695 (1970).

Govind, R., and G. J. Powers, "Control System Synthesis Strategies," *AIChE 82nd National Meeting*, Atlantic City, NJ (1976).

Ishida, C., "An Approach to Optimal Process Plant Operation," Japan-US Joint Seminar, Kyoto Japan (June 23, 1975).

Joseph, B., and C. Brosilow, "Inferential Control of Processes," *AIChE J.*, **24**, 485 (1978).

Kaiser, V. A., J. D. Mahoney, T. M Stout, "An Optimum Approach to Optimization," *ISA*, 3.3-1-66 (Oct., 1966).

Kuehn D. R., and H. Davidson, "Computer Control II. Mathematics of Control," *Chem. Eng. Prog.*, **57**, No. 6, 45 (June, 1961).

Kurihara, H., "Optimal Control of Fluid Catalytic Cracking Processes," ScD Thesis, M.I.T. (1967).

Latour, P. R., "Comments on Assessments and Needs," *AIChE Symp.*, Ser. 159, **72** (1976).

Lee, W., and W. V. Weekman, Jr., "Advanced Control Practice in the Chemical Process Industry: A View from Industry," *AIChE J.*, **22** (1976).

Lefkowitz, I., "Systems Control of Chemical and Related Process Systems," *6th IFAC Congress*, Boston, MA (1975).

Maarleveld, A., and J. E. Rijnsdorp, "Constraint Control on Distillation Columns," *Automatica*, **6**, 51 (1970).

Morari, M., "Studies in the Synthesis of Control Structures of Chemical Processes," Ph.D. Thesis, Univ. of Minnesota (Dec., 1977).

Morari, M., Y. Arkun, and G. Stephanopoulos, "An Integrated Approach to the Synthesis of Process Control Structures," *JACC Proceedings*, Philadelphia, PA (1978).

Pohlenz, J. B., "How Operation Variables Affect Fluid Catalytic Cracking," *Oil Gas J.*, **61** (13), 124 (1963).

Rademaker, O., J. E. Rijnsdorp, and A. Maarleveld, *Dynamics and Control of Continuous Distillation Units*, Elsevier Scientific Publishing Co. (1975).

Rijnsdorp, J. E., "Chemical Process Systems and Automatic Control," *Chem. Eng. Prog.*, **63**, No. 7, 97 (July, 1967).

Shah, M. J., and R. E. Stillman, "Computer Control and Optimization of a Large Methanol Plant," *Ind. and Eng. Chem.*, **62**, No. 12, 59 (Dec., 1970).

Umeda, T., and T. Kuriyama, "A Logical Structure for Process Control System Synthesis," *IFAC Congress*, Helsinki, Finland (1978).

Webb, P. U., B. E. Lutter, and R. L. Hair, "Dynamic Optimization of FCC Units," *AIChE Annual Meeting*, New York (1977).

Weber, R., and C. Brosilow, "The Use of Secondary Measurements to Improve Control," *AIChE J.*, **18**, 614 (1972).

Westerberg, A. W., and C. J. DeBrosse, "An Optimization Algorithm for Structured Design System," *AIChE J.*, **19**, 335 (1973b).

Manuscript received July 23, 1979; revision received April 21, and accepted May 7, 1980.

Analysis of Drop Size Distributions in Lean Liquid-Liquid Dispersions

GANESAN NARSIMHAN
DORAISWAMI RAMKRISHNA
School of Chemical Engineering
Purdue University
West Lafayette, Indiana 47907

JAI P. GUPTA
Department of Chemical Engineering
Indian Institute of Technology
Kanpur, 208016, India

Experimental measurements of transient drop size distributions in a stirred liquid-liquid dispersion (with low dispersed phase fraction) have been used concomitantly with population balance theory to recover the transition probability of droplet breakage, based on a similarity concept. The data remarkably uphold the proposed similarity hypothesis, and the estimated probability function displays the same qualitative trend as the model due to Narsimhan et al. (1979).

SCOPE

The analysis of rate processes in liquid-liquid dispersions (as in other dispersed phase systems) is complicated by their dependence on the dynamics of droplet breakage and coalescence and rate processes occurring in single droplets. The framework of population balances is ideally suited to this task, provided certain essential implements of the analysis are properly identified. These implements are transition probability (or simply rate) functions characterizing random droplet breakage and

Correspondence concerning this paper should be addressed to Doraiswami Ramkrishna.

0001-1541-80-3821-0991-$01.15.